Journal of Medicinal Chemistry

Article

Identification and Optimization of Pyrrolo[3,2-d]pyrimidine Toll-like Receptor 7 (TLR7) Selective Agonists for the Treatment of Hepatitis B

David Craig McGowan, Florence Herschke, Frederik Pauwels, Bart Stoops, Ilham Smyej, Stefaan Last, Serge Pieters, Werner Embrechts, Mourad Daoubi Khamlichi, Tine Thoné, Bertrand Van Schoubroeck, Wendy Mostmans, Debbie Wuyts, Dorien Verstappen, Annick Scholliers, Dorien De Pooter, Deborah Dhuyvetter, Herman Borghys, Marianne Tuefferd, Eric Arnoult, Jin Hong, Gregory Fanning, Jacques Bollekens, Vijay Urmaliya, Ard Teisman, Helen Horton, Tim H.M. Jonckers, and Pierre Jean Marie Bernard Raboisson

J. Med. Chem., **Just Accepted Manuscript** • DOI: 10.1021/acs.jmedchem.7b00365 • Publication Date (Web): 03 Jul 2017

Just Accepted

ACS Publications

Journal of Medicinal Chemistry is published by the American Chemical Society. 1155 Sixteenth Street N.W., Washington, DC 20036

Identification and Optimization of Pyrrolo[3,2-*d*]pyrimidine Toll-like Receptor 7 (TLR7) Selective Agonists for the Treatment of Hepatitis B

David C. McGowan,[*,†] *Florence Herschke,*[*,†] *Frederik Pauwels*,[†] *Bart Stoops,*[†] *Ilham Smyej,*[†] *Stefaan Last,*[†] *Serge Pieters,*[†] *Werner Embrechts,*[†] *Mourad Daoubi Khamlichi,*[‡] *Tine Thoné,*[†] *Bertrand Van Schoubroeck,*[†] *Wendy Mostmans,*[†] *Debbie Wuyts,*[†] *Dorien Verstappen,*[†] *Annick Scholliers,*[†] *Dorien De Pooter,*[†] *Deborah Dhuyvetter,*[†] *Herman Borghys,*[†] *Marianne Tuefferd,*[†] *Eric Arnoult,*[§] *Jin Hong,*[|] *Gregory Fanning,*[†] *Jacques Bollekens,*[†] *Vijay Urmaliya,*[†] *Ard Teisman,*[†] *Helen Horton,*[†] *Tim H.M. Jonckers,*[†] *Pierre Raboisson*[†]

[†]Janssen Pharmaceutica, N.V. Turnhoutseweg 30, 2340 Beerse, Belgium

[§]Janssen Research & Development L.L.C., 1400 McKean Rd, Spring House, PA 19454

[‡]Villapharma Research S.L., Parque Tecnológico de Fuente Álamo. Ctra. El Estrecho-Lobosillo, Km. 2.5- Av. Azul 30320 Fuente Álamo de Murcia, Murcia, Spain

[±]Alios Biopharma, Inc., 260 East Grand Ave., South San Francisco, CA 94080

KEYWORDS

TLR, Toll-Like Receptor; Interferon, IFNα; pyrrolo[3,2-*d*]pyrimidine, HBV

ABSTRACT

Pyrrolo[3,2-*d*]pyrimidines were identified as a new series of potent and selective TLR7 agonists. Compounds were optimized for their activity and selectivity over TLR8. This presents an advantage over recently described scaffolds that have residual TLR8 activity, which may be detrimental to the tolerability of the candidate drug. Oral administration of the lead compound **54** effectively induced a transient interferon stimulated gene (ISG) response in mice and cynomolgus monkeys. We aimed for a high first pass effect, limiting cytokine induction systemically, and demonstrated the potential for the immunotherapy of viral hepatitis.

INTRODUCTION.

Chronic hepatitis B affects over 350 million people worldwide, as it may eventually lead to cirrhosis, or hepatocellular carcinoma (HCC), responsible for one million deaths every year.[1,2] Under 1 in 10 patients achieve functional cure, defined as HBsAg loss and sustained HBV-DNA suppression with or without the appearance of HBsAb (seroconversion), with the approved treatments, nucleosides/nucleotides and interferon-α (IFNα).[3,4,5] Low cure rates are due to high viral antigen loads, inability of the host immune system to control HBV and the immunosuppressive environment of the liver.[6,7]

IFNα therapy, unlike nucleosides/nucleotides, has the potential to control all three issues when directly exposed to hepatocytes and liver nonparenchymal cells. IFNα treatment of HBV-infected hepatocytes, which induces the expression of interferon-stimulated genes (ISG),[8] decreases both HBsAg and HBeAg levels.[9] IFNα also induces the maturation of myeloid dendritic cells towards a Th1 immune-response, which is key to control HBV.[10] The major

reason for the limited clinical use is the intramuscular route of administration, leading to local and systemic exposure of exogenous recombinant IFNα responsible for both injection site and systemic side effects.[10]

Conversely, orally administered agents inducing endogenous IFNα, like TLR7 agonists, could be more potent and better tolerated.[11] Toll Like Receptors (TLRs) play an important role in human innate immunity by recognizing pathogen associated molecular patterns (PAMPs) present in a variety of viruses and microorganisms.[12,13,14] TLR7 recognizes foreign genetic material in the form of single-stranded viral RNA. The receptor is localized in the endosome of plasmacytoid dendritic cells (pDC), and B lymphocytes.[15,16] Detection of foreign nucleic acid in pDCs leads to an antiviral immune response, resulting in an abundant production of endogenous IFNα, and leading to the transcription of interferon stimulated genes (ISGs).[8,15,16] In B cells, activation of TLR7 induces B cell maturation and secretion of antibodies which could promote HBsAg seroconversion.[17,18] TLR8 shares a similar protein structure, is also involved in the detection of viral RNA, but differs in that it is found to be expressed on myeloid dendritic cells and monocytes rather than on pDC and B cells.[19] TLR8 agonism may have the advantages of a strong Th1 response, but may suffer drawbacks such as the induction of pro-inflammatory cytokines.[20] This manuscript focuses on the effort towards an oral, small-molecule TLR7 selective agonist with a high first pass effect would limit IFNα levels in the plasma, resulting in a pre-systemic immune modifying response that could be beneficial toward the treatment of chronic HBV.

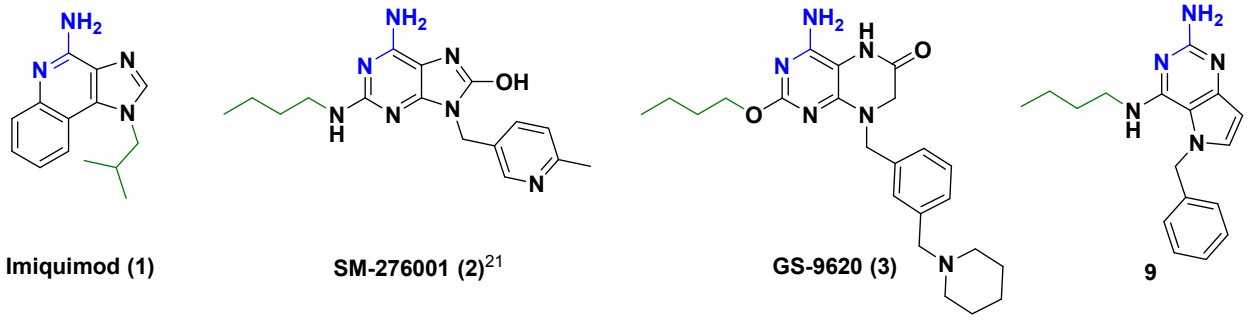

Figure 1. Described TLR 7 agonists and novel pyrrolo[3,2-*d*]pyrimidine (**9**).

There are several TLR7 agonist series described to date, some examples are shown in Figure 1. Imiquimod (**1**), is a marketed medication to treat actinic keratosis and basal cell carcinoma.[22] A second example TLR7 selective agonist from the literature is **2,** of the 8-hydroxy-adenine series, described as a potent IFN inducer in both mice and monkeys.[21]The pteridone series of agonists, represented by GS-9620 (**3**), was examined in clinical trials to treat HBV.[11] A cynomolgus monkey study performed with **3** has demonstrated that an oral dose of 2 mg/kg resulted in a C_{max} that was 2-fold lower than that achieved following i.v. infusion of 0.1 mg/kg **3**. However, mean IFNα plasma levels induced following oral dosing were greater than 60-fold higher than that produced by i.v. infusion.[23]Drug candidates having a rapid elimination after oral administration would potentially improve the overall tolerability and limit the risk for tachyphylaxis, this was indeed one objective in this program. Another objective was to maximize the selectivity of the TLR7 agonist series over TLR8, to limit the induction of pro-inflammatory cytokines (e.g. TNFα). Indeed, **3** has been reported to be 30-fold selective for human TLR7 vs TLR8.[24]

A structural observation of known TLR 7 agonists from Figure 1 reveals several common aspects. They all contain, at minimum, a bicyclic core scaffold, with an aryl group pendant, or fused as in Imiquimod. Contained in the core structure is a minimal pattern of a nitrogen hydrogen bond acceptor, and an adjacent, unsubstituted NH_2 hydrogen bond donor. A third

common aspect is the hydrophobic tail, typically four carbon atoms, connected by an oxygen or nitrogen atom, and positioned three to four bonds away from the aryl group. If indeed there is a recognition element of the TLR7 protein toward RNA bases then perhaps new scaffolds would best imitate the shape and electrostatics of adenine and guanine. The design of pyrrolo[3,2-*d*]pyrimidine (**9**) started from the concept to use the core pyrimidine scaffold of previously described TLR agonists,[25,26]keeping the hydrogen bond donor and acceptor pattern of the pyrimidine and adding a fused ring so that the pendant benzyl group was placed proximal to the alkyl chain. Among the many permutations attempted in our laboratory, we would like to focus this manuscript on the success of the TLR7 selective pyrrolo[3,2-*d*]pyrimidine series starting from the initial compound synthesized (**9**). Indeed, this novel structure holds all three of the desired design attributes. The butyl chain and pendant benzyl group project ipsilaterally from the bicyclic aromatic scaffold containing a similar donor acceptor pattern as the described agonists in Figure 1.

We employed two *in vitro* assays to assess the activity of compounds during the SAR exploration. In the first in vitro assay, the ability of compounds to agonize human TLR7 and TLR8 was assessed in a cell-based reporter assay using HEK293 cells transiently transfected with a wild-type TLR7 or TLR8 expression vector and a NFκB-luc reporter construct. To confirm the activity compounds were tested in the second *in vitro* assay, using IFN-mediated anti-HCV activity in the replicon system upon incubation with conditioned media from human peripheral blood mononuclear cells (hPBMCs). In this assay, activation of human TLR7 on pDCs results in the production of IFN. Promising derivatives were evaluated in rat pharmacokinetic studies and a mouse pharmacokinetic-pharmacodynamic model. The selected

lead candidate was tested in the mouse hydrodynamic injection (HDI) model and finally in cynomolgus monkey.

MEDICINAL CHEMISTRY STRATEGY

Our strategy was to systematically investigate the structure activity relationship of this novel series of pyrrolo[3,2-*d*]pyrimidines, which was divided into three sub-series. The initial sub-series, represented by analogues **9** to **27** (Table 1), where the *n*-butyl amine was conserved and the phenyl ring is replaced by aliphatic and heterocyclic substituents, was designed to optimize activity and selectivity toward TLR7. The second sub-series (compounds **28** to **45**) allowed the exploration of alternatives to the aliphatic amine. Finally, in the third sub-series (compounds **46** to **59**), to afford selective TLR7 agonists with limited off-target activity, the nitrogen atom of **42** was replaced with an oxygen that afforded the lead compound **54** for further evaluation. In the context of this project, and in contrast to a traditional medicinal chemistry program, rapidly metabolized compounds were desired, thus limiting compound exposure and systemic cytokine activation. Furthermore, it has been demonstrated that a robust anti-viral response can be achieved in non-human primates with less than daily dosing of a TLR7 agonist.[27] Despite the expected low compound plasma concentrations, an effort was made to remove off-target activity including, for example, the potential to inhibit the hERG potassium ion channel.

CHEMISTRY

The synthesis of this series of pyrrolo[3,2-*d*]pyrimidines is depicted in Scheme 1 and began with 2,4-dichloropyrrolo[3, 2-*d*]pyrimidine (**4**). Alkylation with benzyl bromide in DMF afforded *N*-benzyl analogue **5** in 50% yield. Displacement of the first chlorine atom with *n*-butylamine in 1,4-dioxane afforded **6** in a modest 67% yield. On the side, the 2-chlorine was converted to a

hydroxyl group by heating in aqueous acetic acid to afford **7**. Finally, nucleophilic aromatic substitution at the 2-chlorine with sodium azide in a mixture of NMP/water afforded the 2-azido intermediate **8**, followed by a Staudinger reduction provided the initial agonist **9** after purification via silica gel column chromatography.[28]

For later analogues, the synthesis was ameliorated to a more scalable route, avoiding the hazardous use of azides and high temperature microwave reaction.[29] Scheme 2 depicts an example of the synthetic pathway starting with the condensation between ethyl 3-amino-1*H*-pyrrole-2-carboxylate and 1,3-bis(methoxycarbonyl)-2-methyl-2-thiopseudourea, analogous to methods described in the literature.[30] The resulting 4-hydroxy-pyrrolo[3,2-*d*]pyrimidyl carbamate (**10**) was converted to the 4-chloro-pyrrolo[3,2-*d*]pyrimidinyl carbamate (**11**) via phosphorus oxychloride in 46% yield. Alkylation of the pyrrole nitrogen under standard Mitsunobu conditions proceeded in moderate yield (65%) to afford **12**. This was followed by base mediated deprotection of the 2-amino carbamate (**13**) and finally displacement of the chlorine by an amine nucleophile in a polar solvent provided **37**, or by an oxygen nucleophile, as in the third sub-series, facilitated by NaH (e.g. **55)**.

Scheme 1. Representative Synthetic Route of Pyrrolo[3,2-*d*]pyrimidines.[a]

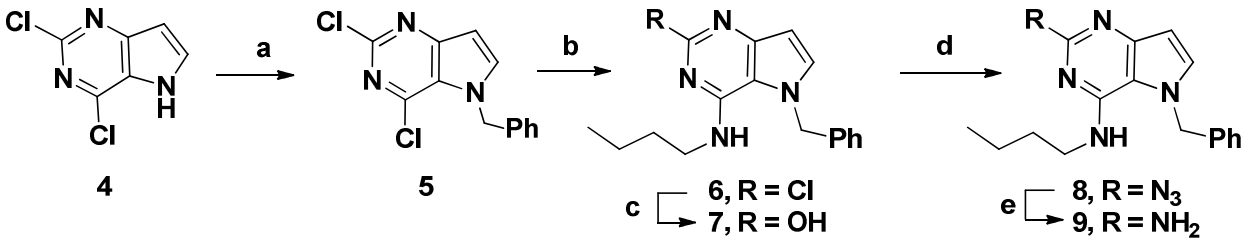

[a]Reagents and conditions: (a) BnBr, Cs_2CO_3, DMF, 70ºC, 50% isolated yield; (b) *n*-butylamine, 1,4-dioxane, 100ºC, 67% yield; (c) HOAc, aq. HCl, 100ºC, 24h, 40%; (d) NaN_3, NMP/H_2O: 9/1, microwave 170ºC, 5h, 86%; (e) PPh_3, 1,4-dioxane:H_2O 9:1, 120ºC, 16h, 76%.

Scheme 2. Representative Alternate Synthesis of Pyrrolo[3,2-*d*]pyrimidines.[a]

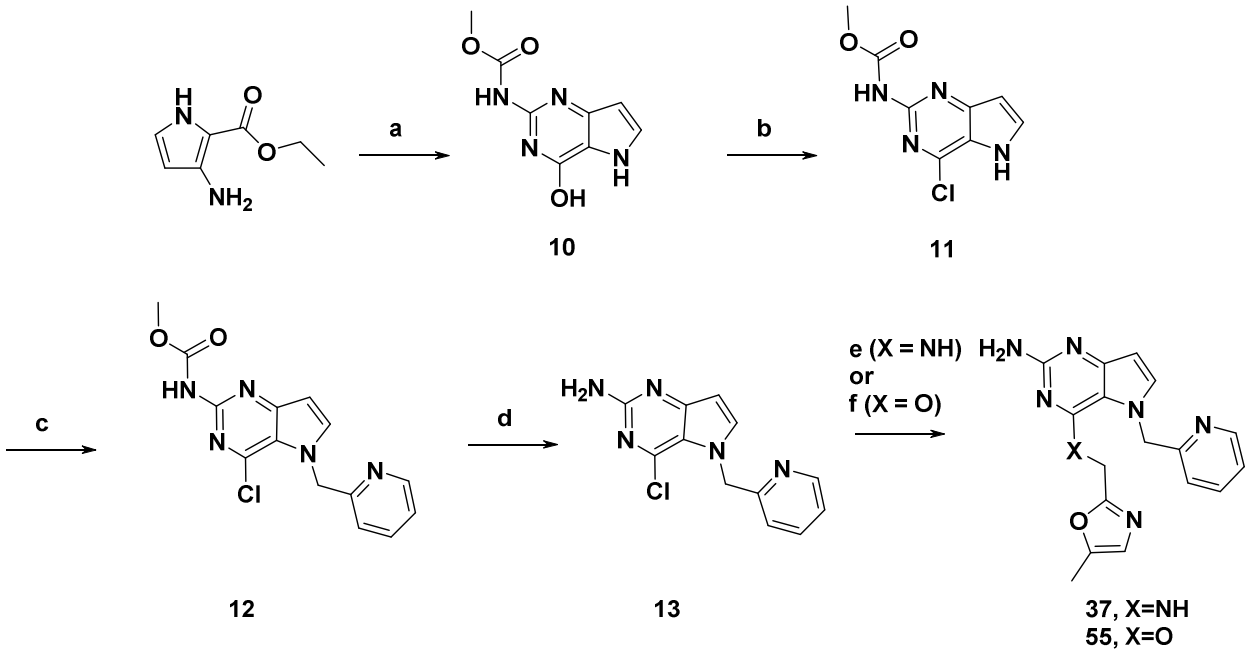

[a]Reagents and conditions: (a) 1,3-bis(methoxycarbonyl)-2-methyl-2-thiopseudourea, HOAc, $NaOCH_3$, CH_3OH, rt, 16h, 87%; (b) $POCl_3$, DIPEA, ACN, 70ºC, 1h, 46%; (c) 2-pyridylmethanol, PPh_3, DIAD, THF, rt, 30 min., 65%; (d) NaOH, 1,4-dioxane, 60ºC, 5h, 75%; (e) 5-methyl-2-oxazolemethanamine, DMSO, 110ºC, 16h, 15%; (f) (5-methyloxazol-2-yl)methanol), NaH, THF, 0 to 50ºC, 30 min., 22%. See WO2014056953 and WO2014207082.

RESULTS AND DISCUSSION

Structure-Activity Relationship. Changes in the 2-amino group led to inactivity (e.g. **7, 8** were > 25 μM [hTLR7, 8]) and so further modifications were not pursued. The first example, having an unsubstituted phenyl ring and an *n*-butyl carbon chain (**9**) showed exceptional TLR7 activity, but unsatisfactory selectivity over the hERG receptor (IC_{50} = 2.1 μM). When the phenyl group was more distal to the scaffold (e.g. **14, 15**) TLR7 potency resulted in the same range as **9**, however undesired TLR8 activity was observed. Replacement of the phenyl group of **9** with an amide led to lower activity (**16**), but improved with the isobutene replacement (**17**). The thiophene analogue **18** had TLR7 selectivity superior to **9** in contrast to the 2-thiazole congener **19** with a selectivity ratio of only 12. The imidazo[1,2-*a*]pyridine fragment (**20**) and the three pyridine analogs **21** to **23** demonstrated that TLR7 activity was gained when the nitrogen of the heterocycle was adjacent to the methylene group. This substitution pattern showed that the

pyridine ring could be modified (**24-26**) and still retain TLR7 selectivity with the exception for the 2-pyridyl-6-methoxy analogue (**27**) that exhibited outstanding potency on TLR7, but carried undesired TLR8 activity. Indeed, **21** displayed remarkable activity and selectivity, and lower CYP450 inhibition than the phenyl (**9**) or thiophene (**18**) congeners (see supporting information) and would be held constant for exploration in the following subseries. In addition, extensive possibilities exist to access substituted pyridines, facilitating future SAR exploration.

Table 1. The Structure Activity Relationship of Benzyl Group Replacements.[a]

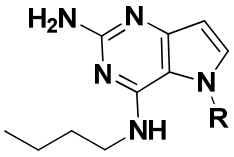

Entry	R	Human TLR7 (LEC[b] μM)	Human TLR8 (LEC[b] μM)	Selectivity Ratio	hPBMC (μM)
9	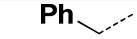	0.23	>25	>109	0.1
14	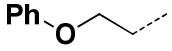	0.07	1.16	5	0.06
15	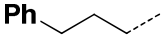	0.16	3.78	24	0.06
16	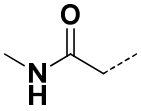	6.95	>25	>5	1.0
17	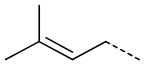	0.4	>25	>63	0.22
18	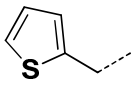	0.13	>25	>192	0.03
19	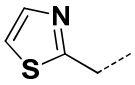	0.19	2.27	12	0.13
20	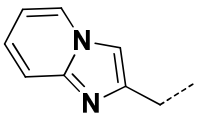	0.15	>25	>167	0.04
21	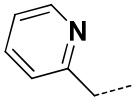	0.15	>25	>167	0.06

22	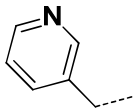	1.36	>25	>18	0.26
23	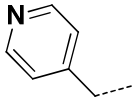	1.53	>25	>16	0.75
24	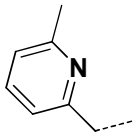	0.08	>25	>313	<0.01
25	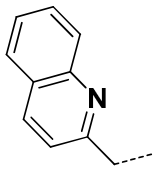	0.3	>25	>83	0.28
26	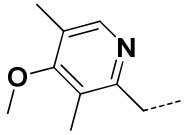	0.18	>25	>139	0.14
27	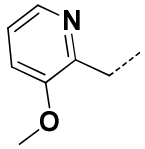	0.008	0.59	74	<0.01

[a]All compounds had a CC_{50} > 24 μM in the HEK 293 cytotoxicity assay (see supporting information).[b]LEC; least effective concentration values were averaged when determined in two or more independent experiments. See supporting information.

The subsequent subseries of analogues would focus on systematic changes of the amine group. Variation of the amine while holding the unsubstituted pyridyl group constant is described in Table 2. Differences in activity were seen when the butyl chain was replaced by other aliphatic or heteroaromatic groups, all were selective for TLR7 over TLR8. An ether variation on the butyl chain of **21** displayed a loss of activity (**28**)**.** The same held true for alkyl ethers **29** and **30**. A modest decline in activity for aminoalcohol **31** was observed when compared to **21,** but highlighted that a polar group was well tolerated. Heterocyclic substituents presented a range of activity depending on the ring size and position of the heteroatoms. The bis-pyridyl analogues

(**32**, **33**) did not show an increase in potency over the butyl chain, and furthermore the racemic alpha-methyl group of **33** did not display a favorable increase in activity and so further modifications were not pursued. In contrast, thiazole and 1,3,4-oxadiazole (**34, 35**) ring modifications were deleterious to activity, suggesting that the electrostatic properties of the ring are important in addition to the regiochemisty of the heterocycle. The oxazoles displayed higher potency when the methyl group was placed next to the oxygen (**37**), as opposed to neighboring the nitrogen atom (**38**). Both oxazoles showed binding to the serotonin receptors (e.g. IC_{50} 5HT2a = 0.65 and 2.3 μM, respectively). The methyl isoxazole **42** was an equipotent TLR7 agonist and had less inhibition of the 5HT2a receptor (IC_{50} = 6.2 μM). The cyclopropyl congener (**43**) was also an effective agonist, but displayed more potent hERG inhibition than **42** (hERG IC_{50} = 0.2 vs. 1.2 μM respectively). Finally, if the N-O bond in the isoxazole was reversed (**45**) then potency was lost.

Table 2. Structure Activity Relationship of Amine Substitution.[a]

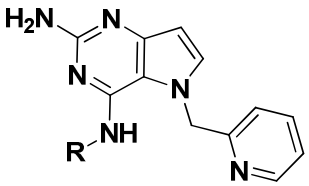

Entry	R	hTLR7 (LEC[b] μM)	hPBMC (μM)
28	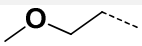	1.81	2.2
29	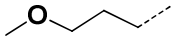	4.45	0.5
30	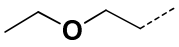	1.24	0.5
31	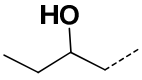	0.43	0.05
32	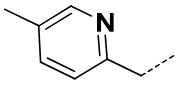	0.4	0.07

		R_1	R_2	X		
33	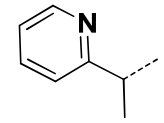				0.26	0.04
34	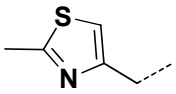				6.13	2.2
35	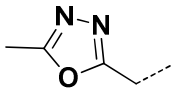				1.24	0.09
36	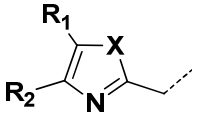	H	H	O	0.52	0.13
37		CH_3	H	O	0.06	0.006
38		H	CH_3	O	1.16	0.15
39		H	H	S	3.04	0.56
40		CH_3	H	S	0.06	0.009
41	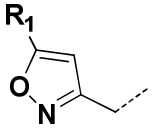	H			0.9	0.42
42		CH_3			0.04	0.006
43		△			0.05	0.008
44		iPr			0.34	0.02
45	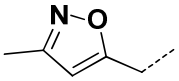				0.49	0.13

[a]All compounds were > 25 μM LEC [hTLR8], and CC_{50} > 24 μM in the HEK 293 cytotoxicity assay described in the supporting information. [b]LEC; least effective concentration values were averaged when determined in two or more independent experiments. See supporting information.

Compound **42** had achieved the potency and selectivity that was desired and was identified to have no appreciable receptor kinase activity, and no CYP inhibition across several isozymes (see supporting information). However, **42** remained a strong hERG binder (IC_{50} = 1.2 μM).

The strategy to identify the best lead candidate was two-fold: First, the preferred 5-methylisoxazole moiety was held constant allowing the examination of the effect of substituted pyridines, that could influence hERG receptor binding as suggested in the literature.[31] Secondly, it has been described that introduction of an oxygen atom into a aliphatic chain can reduce the propensity of hERG binding.[32] Thus, we explored pyridine ring variations, and converted the amine connection of the heterocycle (Table 3, R_5) to an ether (Table 3, X = O).

Table 3. Modifications to the Heterocyclic Rings.[a]

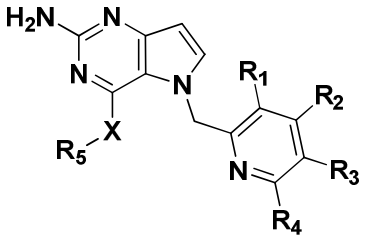

Entry	R_1	R_2	R_3	R_4	X	R_5	Human TLR7 (LEC[b] μM)	hPBMC (μM)	hERG IC_{50} (μM)	cLogP
46	H	H	CH_3O	CH_3O	N	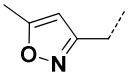	0.003	0.0006	0.7	2.0
47	H	H	H	CH_3O	N	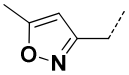	0.006	0.001	2.3	1.9
48	H	H	F	H	N	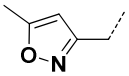	0.070	0.009	2.0	1.3
49	F	H	H	H	N	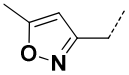	0.086	0.009	2.1	1.3
50	H	H	CF_3	H	N	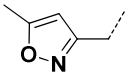	0.050	0.03	0.5	2.1
51	H	CF_3	H	H	N	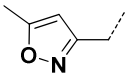	0.050	0.02	n.d.	2.1
52	Cl	H	H	H	N	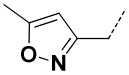	0.050	0.04	0.9	1.9
53	H	Cl	H	H	N	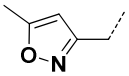	0.050	0.02	0.5	1.9
54	H	H	H	H	O	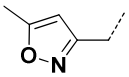	0.4	0.061	>50	1.1
55	H	H	H	H	O	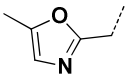	0.6	0.10	>50	0.8
56	H	H	H	H	O	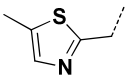	0.8	0.099	44.7	1.7
57	H	H	H	H	O	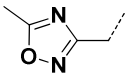	6	1.96	>50	0.5
58	CH_3O	H	H	H	O	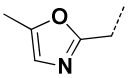	0.07	0.006	2.2	1.3
59	CH_3O	H	H	H	O	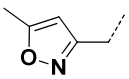	0.03	0.006	1.6	1.6

[a]All compounds were > 25 μM LEC [hTLR8], and showed CC_{50} > 24 μM in the HEK293 cytotoxicity assay described in the supporting information. [b]LEC values were averaged when determined in two or more independent experiments. n.d., not done.

Variations in the pyridine substitution (compounds **46** to **53**) afforded several potent agonists, especially when substituted by electron rich moieties (**46, 47**). It is described in the literature that within a given series of compounds there can be a correlation between hERG binding and a measurement of lipophilicity such as cLogP.[33] However, within this chemical series, there was a weak correlation between cLogP and hERG IC_{50}. On the contrary, the best progress in avoiding hERG inhibition came with the discrete structural modification of **42** to the corresponding ether **54**, despite the two compounds having nearly the same cLogP of 1.1. This modification led to an improved cardiovascular safety profile with a minor loss in TLR7 potency. Further heterocyclic ether variants (oxazole **55**, thiazole **56**, oxadiazole **57**) also bore relatively no hERG inhibition and had intriguing differences in potency that may be rationalized by their difference in charge distribution.

The electrostatic potential alignment of analogs **54** to **57** showed that the most potent compounds share a similar electrostatic profile (Figure 2, see supporting information). There are two positions on the ring on either side of the methylene group that are key. One alpha position (South side, Figure 2) can be electronegatively charged, while the other (North side) must be electropositively charged (thiazole) or neutral as the potency decreases when this side of the molecule becomes strongly electronegative, as in oxadiazole derivative **57**. The electrostatic profile of the best substituent could be used as a signature for further exploration of this series. Finally, substituted pyridines **58** and **59** once again displayed that potency could be regained by the addition of electron donating methoxy groups on the pyridine ring, but unfortunately afforded decreased selectivity over the hERG antitarget.

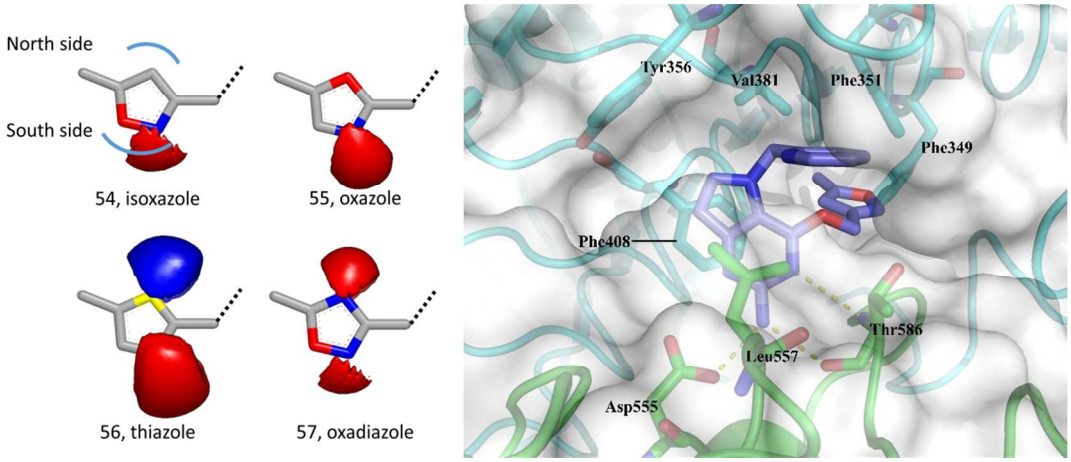

Figure 2. Left: Electrostatic potential comparison, based on AM1-BCC charges, between isoxazole (**54**), oxazole (**55**), thiazole (**56**), and oxadiazole (**57**). Right: Predicted binding mode by docking (Glide XP) for compound **54** in a monkeyTLR7 structure (one TLR7 monomer in cyan and the other in green). See supporting information.

The binding mode of **54**, obtained by docking into monkey TLR7 (see supporting information), illustrated in Figure 2, corresponds to the expected binding mode and is comparable to the binding mode described for Resiquimod.[34]

Strong, direct dual hydrogen bonds between the 2-amino group of **54**, the acidic side chain of Asp555, and the backbone of Thr586 (Carbonyl) were observed. An additional H-bond between the 3-position of the pyrimidine and the backbone of Thr586 (Amino) contributes to the stabilization of the compound in the binding site. The scaffold is further stabilized by a π-stacking interaction with Phe408 on one side, and by CH-π interactions with Leu557 on the other side.

The methylisoxazole is deeply buried in the hydrophobic pocket formed by residues Phe349, Phe351, Val381 and Ile585, stabilized by a π-stacking interaction with Phe351, and has good surface complementarities. In addition, the pyridine ring of **54** has a CH-π interaction with the Cα of Gln354.

In comparison, the binding mode of **54**, is less favorable in hTLR8 for two main reasons (illustrated in figure S1): 1) Leu557 is replaced by Asp545 in hTLR8. The scaffold no longer has a CH-π interaction. Instead, Asp545 is making non-favorable electrostatic interactions with the compound. 2) Thr586 is replaced by Thr574 in hTLR8. The side chain of Thr574 adopts a different orientation, providing less room to accommodate **54**. The Thr574 side chain is making only one H-bond with the 2-amino group instead of two with its backbone in monkeyTLR7. In addition, the Phe351 (TLR7) is replaced by Tyr358 in TLR8 and does not allot enough room to accommodate the methylisoxazole in the hydrophobic pocket. The combination of both a less stable interaction of the scaffold and the methylisoxazole, predicts that **54** would be less potent on hTLR8.

Agonist **54** was found to be selective for TLR7 over TLR8 in the same cellular reporter assay using HEK293 cells transiently transfected with mouse, rat, or cynomolgus TLR7 or TLR8 expression vector and NFκB-luciferase reporter construct (see supporting information). In addition, no direct activation of NFκB was observed. After repeating at higher concentration, **54** was found to be very selective over TLR8 (>100 μM LEC human TLR8).

Table 4. Activity of 54 Across Species *in vitro*.[a]

Transient transfection of HEK293 cells with:	Species	Avg. LEC (μM)
TLR7 + NFκB-luc	Human	0.41
	Mouse	0.34
	Rat	0.33
	Cynomolgus monkey	0.80
TLR8 + NFκB-luc	Human	>100
	Mouse	>25
	Rat	>25
	Cynomolgus monkey	>25
NFκB-luc		>25

[a]see supporting information for n, and confidence interval.

The permeability of **54** was measured in a MDCK-MDR1 cellular assay at 5 μM. **54** displayed decent permeability with a P_{app} (A→B, in the presence of GF120918) of 41 x 10^6 cm s^{-1}, and an efflux ratio of 18, indicating that the compound is a P-gp substrate. **54** demonstrated low inhibition across five CYP450 isozymes (IC_{50} > 10 μM, see supporting information) and was also not a time dependent inhibitor of CYP450 3A4. Table 5 lists the *in vitro* metabolic stability of **54** in liver microsomes and whole-cell hepatocytes across species. Intrinsic clearance (CL_{int}) in liver microsomes was moderate in mouse, dog and human and high in rat and monkey. The intrinsic clearance in hepatocytes evaluated the potential for non-CYP mediated metabolism and was low to moderate in mouse, dog and human and high in monkey and rat. Plasma protein binding across species remained relatively low and ranged from 54 to 63% bound. **54** had limited inhibition of the hERG potassium ion channel ^{3}H-dofetilide binding *in vitro* (IC_{50} > 50 μM), which correlated with a relatively low functional hERG inhibition in the QPatch™ planar patch clamp assay (32% inhibition at 3 μM).[35] To evaluate whether this effect, albeit low, or other undetected compound characteristics could lead to undesired electrophysiology effects *in vivo*, **54** was subjected to a cardiovascular safety pharmacology study in anesthetized female guinea pigs. In this model, electrophysiological changes were measured after administration of **54** by i.v. infusion in pentobarbital anesthetized animals (cumulatively dosed up to 4.9 mg/kg i.v.). From this study, no major cardio-electrophysiological effects were observed up to maximal total plasma exposures of 9700 ng/mL (at the end of the infusion). There was no tendency for the formation of micronuclei *in vitro* in the presence and absence of rat S9 fraction, and no potential for mutagenicity revealed by the AMES II test. In further support of the lead compound, cytokine induction was measured after compound stimulation of whole blood of healthy volunteers *ex vivo* and included IFNα, IFNγ, IL-12p40, and IL-12p70.

Table 5. *In vitro* Metabolic Stability and Plasma Protein Binding of 54.[a]

Species	CL_{int} microsomes (μL/min/mg)	CL_{int} hepatocytes (μL/min/10^6 cells)	Plasma protein binding (% bound)
Mouse	55	19	63
Rat	>346	>277	61
Dog	44	7	62
Cynomolgus monkey	87	80	52
Human	25	6	54

[a]Values were rounded to the nearest whole number.

Pharmacokinetics. Among preclinical species, the *in vitro* metabolism in rat hepatocytes was exceptionally high, and the *in vivo* clearance was predicted to be above rat liver blood flow. A pharmacokinetic study in healthy male Sprague-Dawley rats investigated the exposure of **54** in systemic circulation following intravenous administration at 2.5 mg/kg and in the portal vein, liver and systemic circulation following oral administration of 10 mg/kg. The i.v. clearance correlated well with the *in vitro* clearance, and exceeded rat liver blood flow, resulting in a very short terminal half-life. The maximum concentration in the portal vein was equal to 314 ng/mL and occurred one hour post-dose. The concentration measurements in the liver and systemic circulation were below quantifiable limits. Oral administration in dogs (1 mg/kg) resulted in fast absorption (T_{max} at 0.5 h, first sampled time point). The C_{max} was 125 ng/mL and the systemic concentration dropped below 10 ng/mL, 4 hours post administration. The systemic concentration in dog was higher than in rat which is in line with the in vitro stability in microsomes and hepatocytes.

Pharmacokinetic and pharmacodynamic studies in mice and cynomolgus monkeys. A mouse *in vivo* model was used to demonstrate the initial proof of concept to induce endogenous IFNα. Single oral administration of 0.3, 1, 3 and 10 mg/kg doses of **54** were given to healthy, female, fasted C57Bl/6 mice. Concentration of compound and mouse-IFN via ELISA were

measured from the plasma and compared to vehicle. The results are shown in Table 6. **54** was found to be rapidly cleared, in conjunction with our target profile. Both C_{max} and AUC increased less than dose proportionally between 0.3 and 3 mg/kg and more than dose-proportionally between 3 and 10 mg/kg. T_{max} occurred between 0.5 and 1 h, and a liver to plasma ratio of 2 was measured. Levels of IFNα peaked between one and two hours post administration in both plasma and in the liver. Increase in IFNα was dose-proportional in plasma, but sigmoidal in the liver, suggesting a possible saturation of endogenous IFNα production especially in the liver (Table 6). ISG (interferon-stimulated gene) expression was measured in parallel by RT-qPCR. Interestingly, all three *Isg15*, *Oas1b* and *Mx1* were upregulated to a higher level in the liver than in the plasma, while IFNα, *Cxcl10* or the target *Tlr7* were upregulated similarly in blood and liver (Table 6). These data reveal that **54** can induce an antiviral ISG response without inducing an IFNα response at a low dose. One potential drawback of the TLR7 selective agonist **2**, are the significant plasma concentrations observed at 8h in mice after an oral dose of 1mg/kg,[22] in contrast to **54** that was below quantifiable limits at the same dose and timepoint. Therefore, compound **54** has rapid clearance after oral administration in mice, limiting compound exposure and systemic cytokine activation, resulting in an improved potential tolerability profile.

Table 6. Mean Maximum Levels in the Plasma and Liver and ISG upregulation, induced by 54 after oral dosing in C57Bl/6 mice.[a]

Dose (mg/kg)	0.3	1	3	10
C_{max} plasma (ng/mL)	3.7	7.1	2.8	72.9
C_{max} liver (ng/g)	6.8	6.3	23.0	152.3
$IFN\alpha_{max}$ plasma (pg/mL)	105	205	560	1365
$IFN\alpha_{max}$ liver (pg/g)	BQL	55	470	580
$Oas1b_{max}$ plasma[b]	1.85	2.1	2.45	2.2
$Oas1b_{max}$ liver[b]	16	14	11	14
$Isg15_{max}$ plasma[b]	1.35	2	1.95	1.75
$Isg15_{max}$ liver[b]	10	60	75	100
$Mx1_{max}$ plasma[b]	12	18	20	19
$Mx1_{max}$ liver[b]	60	315	745	775
$Tlr7_{max}$ plasma[b]	3.6	3.7	4.05	4.15

Tlr7$_{max}$ liver[b]	3.15	2.45	2.9	3.7

[a]Groups of 9 mice were dosed with 0.3, 1, 3 or 10 mg/kg of **54** At 0.5 hours, blood was drawn to quantify compound. At 1, 2, or 4 hours, three mice of each group were sacrificed and blood was drawn to measure plasma and liver compound levels (by LC-MS), IFNα (by ELISA) and ISG expression levels (by RT-qPCR). Values were rounded to the nearest whole number. BQL, below quantifiable limit; [b]fold-change relative to vehicle.

The potential of **54** to inhibit HBV replication *in vivo* was tested in the hydrodynamic injection (HDI)-HBV mouse model. This model allows an initial assessment of the anti-HBV activity, as mice develop an acute infection which is cleared within two weeks.[36] **54** was administered orally to C57Bl/6 male mice one day after HDI, for five consecutive days at 0.3, 1, 2.5, and 5 mg/kg QD and was found to be well tolerated (no clinical observations were noted). The dose was chosen based on the robust ISG upregulation observed in healthy C57Bl/6 mice (Table 6). **54** induced a 2.7 log decrease in serum HBV viral load from 0.3 mg/kg, and a maximum 3.1 log decrease was observed for doses between 1 and 5 mg/kg (Figure 3). Also, one day after the last dose, mice were sacrificed to evaluate liver HBV viral load (Figure 3). A small but statistically significant (One-way ANOVA with Dunnett's multiple comparison) decrease was observed at all doses, and was maximal for the 5 mg/kg dose (0.63 log decrease). In contrast, a similar decrease in viral load, in either the serum or the liver, required a higher dose of **3** (20 mg/kg).

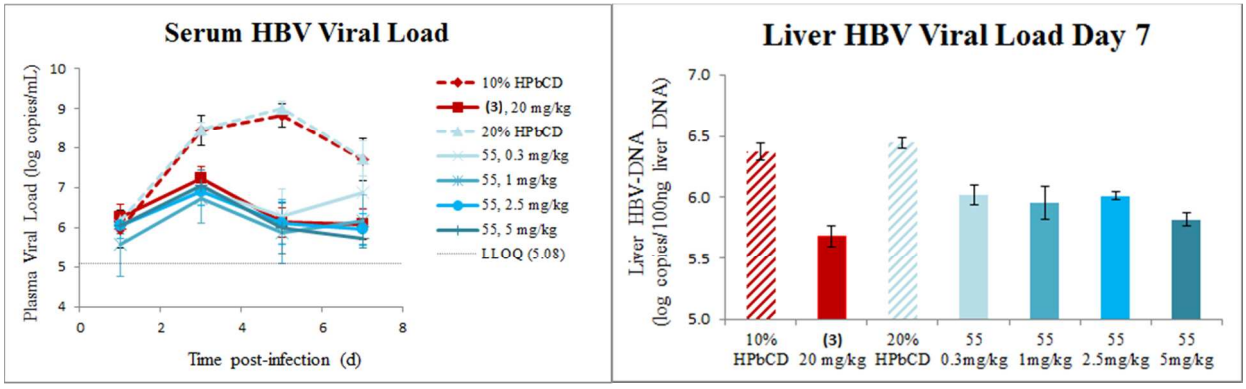

Figure 3. Efficacy of **54** in the HDI-HBV mouse model. Left: Serum HBV viral load over time (mean +/- SD). Right: Liver HBV viral load at end of dosing (qPCR, mean +/- SD). Seven groups of eight male C57Bl/6 mice, 4-6 weeks old, were administered 20 µg of pAAV2-HBV1.3mer genotype D plasmid by hydrodynamic injection. 1 day later, groups 1 to 7 received compound **54** orally at 0, 0.3, 1, 2.5, and 5 mg/kg QD, respectively, for 5 days. HPbCD20% at acidic pH was used as vehicle. At different time points, blood was sampled to measure serum HBV

viral load by qPCR. 1 day after the last dose, mice were euthanized to measure liver HBV viral load by qPCR. LLOQ, lower limit of quantification.

Healthy cynomolgus monkeys were chosen as the next preclinical pharmacokinetic-pharmacodynamic model, as they are the closest available model to human immunology.[37] Oral doses of 1, 3 and 10 mg/kg of **54,** were well tolerated (no clinical observations and no relevant change in body weight, body temperature observed). Maximum mean plasma concentration occurred at 0.25 to 2 hours post dose and increased dose-proportionally, despite the large variability observed. The low oral bioavailability (<1% F) can potentially be attributed to a high first pass effect, assuming that absorption was similar to that generated in the rat hepatic portal vein pharmacokinetic study. According to the mode of action, a transient and dose-dependent decrease in lymphocyte counts and increase in neutrophil counts was observed from 1 mg/kg.[38-40] Cytokines were measured in plasma by Luminex or ELISA. IFNα production was detected in all animals starting from the 3 mg/kg dose, and showed a more than dose-proportional profile of maximum response, despite high inter-individual variability. Interestingly, an ISG response was induced starting from 1 mg/kg: *Isg15*, *Oas1b*, *Oasl*, *Mx1*, *Cxcl11*, *Ifit44l* where upregulation (measured by microarray) was detected from 1 mg/kg and peaked at four to eight hours post-dose. A second wave of gene induction was observed at 72 hours post-dose, including ISG *Cxcl10*, as well as monocyte-induced *Ccl18*. Monocyte activation was also suggested by the production of MCP1 (from 1 mg/kg) and IL-1Ra (from 3 mg/kg). General proinflammatory cytokines IL-6 and G-CSF were measurable from 10 mg/kg, while anti-inflammatory cytokine IL-10 was induced from 3 mg/kg. This is encouraging in regards to the safety of compound **54**. Overall, these results demonstrate that **54** is more than simply an interferon inducer and warrant further evaluation for HBV indications.

Table 7. Mean Plasma Pharmacokinetic and Pharmacodynamic Parameters of 54 in Cynomolgus Monkey Following Administration by Oral Gavage.[a]

Dose (mg/kg)	1	3	10
C_{max}(ng/mL)	4.12	11.2	23.4
T_{max}(h)	1-2	0.5-2	0.5-2
$AUC_{0\text{-last}}$(ng.h/mL)	NA	26.7	57.5
IFNα max[a]	BQL	120 (3/5)	2980 (5/5)
MCP1 max[a]	325 (2/5)	1560 5/5)	8295 (5/5)
IL-1Ra max[a]	75 (5/5)	1820 (5/5)	10575 (5/5)
IL-6 max[a]	20 (4/5)	10 (3/5)	525 (5/5)
G-CSF max[a]	90 (3/5)	75 (2/5)	120 (4/5)
IL-10 max[a]	20 (3/5)	45 (3/5)	125 (5/5)

[a]pg/mL, frequency; BQL, below quantification limit; NA, not applicable. Five cynomolgus monkeys were administered 1, 3 or 10 mg/kg of **54** by oral gavage. At 0 (pre-dose), 0.25, 0.5, 1, 2, 4, 8, 24, 48 and 72 hours post-dose, blood was sampled to measure compound concentrations in plasma, cytokine levels (by ELISA or Luminex) and gene expression (by microarray). Doses were administered in different animals, but staggered by 3 days for acute toxicity evaluation.

CONCLUSION

In this manuscript, the research on a novel class of TLR7 selective agonists for immunotherapy of hepatitis B was described. This new series of pyrrolo[3,2-*d*]pyrimidines was designed by taking key elements of chemical series previously described in the literature and combining them into a new structure. We found **54** to be potent and selective over other TLRs in preclinical species. Oral administration of **54** was well tolerated *in vivo,* displayed a high first pass effect, and induced an interferon stimulated gene response in both mice and cynomolgus monkeys. This ISG response, was of higher magnitude in the liver, the site of viral infection, than in the periphery in mice. In the HDI-HBV mouse model, **54** reduced viral load in the serum and in the liver. In cynomolgus monkey, **54** did not induce IFNα systemically after a low (1 mg/kg) oral dose, but induced an upregulation of ISGs. In summary, we have identified a series of novel and potent TLR7 agonists and presented data which indicate the potential for the immunotherapy of viral hepatitis.

EXPERIMENTAL SECTION

Intrinsic clearance (CL_{int}) of 54. CL_{int} was determined in mouse, rat, dog, cynomolgus monkey, and human liver microsomes. Incubations were performed at 37°C, at a compound concentration of 1 μM, and a microsomal protein concentration of 0.5 mg/mL. Samples were removed at intervals of up to 60 min and analyzed for the concentration of compound to determine its intrinsic clearance rate. **54** was incubated in mouse, rat, dog, cynomolgus monkey, and human hepatocytes (10^6 cells/mL) at 1 μM for 0, 10, 20, 40, 60 and 120 min. Samples were removed at intervals of up to 120 min and analyzed for the concentration of compound to determine its intrinsic clearance rate.

Plasma Protein Binding. The free fraction in mouse, rat, dog, cyno and human plasma was determined by rapid equilibrium dialysis (RED device, Thermo Fisher Scientific, Geel, Belgium). The RED device consists of a 48 well plate containing disposable inserts bisected by a semipermeable membrane creating two chambers. A 300 μL aliquot of plasma containing test compound at 5 μM was placed one side and 500 μL of phosphate buffered saline (PBS) on the other. The plate was sealed and incubated at 37 °C for 4.5 h. Samples were removed from both the plasma and buffer compartment and analyzed for test compound using a specific LC-MS/MS method to estimate free and bound concentrations.

Permeability and Efflux. The *in vitro* permeability and potential to be transported by P-glycoprotein (P-gp) was determined using an MDCK cell line transfected with human MDR1 (P-glycoprotein). 5 μM **54** was added to the apical (A) or basolateral (B) side of a confluent monolayer of MDCK-MDR1 cells. Apparent permeability in the A→B direction in absence (P_{app} A→B, 5.5 x 10^{-6}cm/s) and presence (P_{app} A→B, 41 x 10^{-6}cm/s) of GF120918 (P-gp inhibitor) and in the B→A direction in absence of GF120918 (P_{app} A→B, 23 x 10^{-6}cm/s) was measured by

monitoring the appearance of the test compound on the opposite side of the membrane using a specific LC-MS/MS method. The efflux ratios (B→A -GF120918/A→B –GF120918) were calculated to determine whether the test compound was a P-gp substrate.

All in vivo studies were performed in AAALAC-accredited sites, and ethical approval by the corresponding ethical committee was obtained.

Chemistry. Reagents and solvents were purchased from commercial sources and used without purification. All final products were > 95% pure. NMR spectra were recorded on a Bruker Avance 400 spectrometer, operating at 400 MHz for ^{1}H NMR and 101 MHz for ^{13}C NMR or a Bruker 360 spectrometer, operating at 360 MHz for ^{1}H NMR and 91 MHz for ^{13}C NMR. Chemical shifts and multiplicity data are given according to the ACS NMR guidelines. High resolution mass spectrometry was performed on a Waters Acquity® IClass UPLC®-DAD and Xevo G2-S QTOF. The samples were run on a Waters BEH C18 (1.7 µm, 2.1 x 50 mm, at 50ºC) column, with a flow rate of 1 mL/min, using reverse phase chromatography with a gradient from 95% A to 5% A in 4.6 min, and held for 0.4 min (A: 95% CH_3COONH_4 6.5 mM + 5% CH_3CN, B: CH_3CN).

5-benzyl-2,4-dichloro-5*H*-pyrrolo[3,2-*d*]pyrimidine (5). Into a 50 mL vial was placed 2,4-dichloro-5*H*-pyrrolo[3,2-*d*]pyrimidine (1 g, 5.32 mmol), DMF (10 mL), DIPEA (2.75 mL, 16 mmol) and benzylbromide (0.7 mL, 5.85 mmol). The vial was sealed and shaken for 16 hours at rt. The reaction mixture was filtered through silica, and the solvent of the filtrate was removed under reduced pressure. The crude was used without further purification in the next step.

5-benzyl-*N*-butyl-2-chloro-5*H*-pyrrolo[3,2-*d*]pyrimidin-4-amine(6). Into a 50 mL round bottom flask equipped with a magnetic stir bar was placed 5-benzyl-2,4-dichloro-5*H*-

pyrrolo[3,2-*d*]pyrimidine (1.4 g, 5.03 mmol), *n*-butylamine (0.59 mL, 6.04 mmol), and 1,4-dioxane (5 mL). The flask was equipped with a reflux condenser and allowed to heat with stirring at 100ºC for 16 h. After cooling to rt, the solvents were removed under reduced pressure. The crude was purified via silica gel column chromatography using a heptane to EtOAc gradient. The best fractions were pooled and the solvents were removed under reduced pressure to afford the titled compound.

5-benzyl-4-(butylamino)-5*H*-pyrrolo[3,2-*d*]pyrimidin-2-ol (7). A suspension of **6** (70mg, 0.22 mmol) in acetic acid (1 mL) and conc. HCl (0.2 mL) was heated in sealed tube at 100ºC for 24 hours. The solvent was removed under reduced pressure and the crude was purified via silica gel column chromatography using a gradient of CH_2Cl_2 to CH_2Cl_2/CH_3OH (95:5). ^{1}H NMR (300 MHz, DMSO-d_6) δ 10.33 (s, 1H), 7.16-7.35 (m, 4H), 6.98 (d, *J*=6.74 Hz, 2H), 6.19 (t, *J*=5.43 Hz, 1H), 5.85 (d, *J*=2.75 Hz, 1H), 5.52 (s, 2H), 3.22-3.30 (m, 2H), 1.23-1.37 (m, 2H), 0.91-1.06 (m, 2H), 0.73-0.80 (m, 3H).

2-azido-5-benzyl-*N*-butyl-5*H*-pyrrolo[3,2-*d*]pyrimidin-4-amine hydrochloride(8). Into a glass vial equipped with a magnetic stir bar was placed 5-benzyl-*N*-butyl-2-chloro-5*H*-pyrrolo[3,2-*d*]pyrimidin-4-amine (1 g, 3.18 mmol), NaN_3 (0.62 g, 9.53 mmol), and NMP: water (9:1, 4 mL). The glass vial was sealed and the mixture was heated with stirring to 170ºC for 5 h. After cooling to rt, the mixture was diluted with EtOAc (20 mL) and washed with water (5 x 15 mL). The organic layer was dried over magnesium sulfate, the solids were removed via filtration and the solvents of the filtrate were removed under reduced pressure. The crude was purified via silica gel column chromatography using a heptane to EtOAc gradient. The best fractions were combined and the solvents were removed under reduced pressure. The product was suspended in 0.5 mL dioxane and to it was added 1 eq. 4N HCl in dioxane at 0ºC . The mixture was stirred for

16 hours at room temperature and then the solvent was removed under reduced pressure to afford the titled compound. LC-MS (M+H) *m/z* = 322. ^{1}H NMR (300 MHz, CHLOROFORM-*d*) δ 7.32-7.42 (m, 3H), 7.18-7.22 (m, 2H), 6.99-7.08 (m, 2H), 6.90 (d, J=3.16 Hz, 1H), 5.51 (s, 2H), 4.95 (br s, 1H), 3.37 (dt, J=5.22, 6.94 Hz, 2H), 1.13-1.26 (m, 2H), 0.98 (qd, J=7.31, 14.90 Hz, 2H), 0.69-0.78 (m, 3H).

5-benzyl-*N*^{4}-butyl-5*H*-pyrrolo[3,2-*d*]pyrimidine-2,4-diamine (9). Into a glass vial equipped with a magnetic stir bar was placed 2-azido-5-benzyl-*N*-butyl-5*H*-pyrrolo[3,2-*d*]pyrimidin-4-amine (100 mg, 0.311 mmol), 1,4-dioxane (4 mL), water (1 mL), and triphenylphosphine (245 mg, 0.93 mmol). The vial was sealed and the mixture heated with stirring to 120ºC for 16 h. After cooling to rt, the solvents were removed under reduced pressure. The crude was purified via silica gel column chromatography using a CH_2Cl_2 to 10% CH_3OH in CH_2Cl_2 gradient. The best fractions were pooled and the solvents were removed under reduced pressure to afford the titled compound. ^{1}H NMR (400 MHz, DMSO-d_6) δ 7.25-7.33 (m, 3H), 7.19-7.25 (m, 1H), 6.95-7.01 (m, 2H), 5.98 (d, *J*=2.86 Hz, 1H), 5.73 (t, *J*=5.50 Hz, 1H), 5.49 (s, 2H), 5.23 (s, 2H), 3.25-3.32 (m, 2H), 1.28-1.39 (m, 2H), 1.04 (qd, *J*=7.39, 15.02 Hz, 2H), 0.73-0.82 (m, 3H).^{13}C NMR (101 MHz, DMSO-d_6) δ 158.8, 151.7, 150.8, 139.4, 133.2, 129.0, 127.8, 126.5, 110.4, 99.7, 52.0, 39.8, 31.5, 19.8, 14.2. ESI-HRMS (TOF) *m/z*: 296.1878 $[M+H]^+$ (Calcd. for $C_{17}H_{21}N_5$: 295.1797).

Methyl (4-hydroxy-5*H*-pyrrolo[3,2-*d*]pyrimidin-2-yl)carbamate (10). Amino-2-ethoxycarbonylpyrrole hydrochloride (25.8 g, 135.7 mmol) was partitioned between CH_2Cl_2 and sat., aq. $NaHCO_3$, the organic layer was dried over $MgSO_4$, the solids were removed by filtration, and the filtrate evaporated to dryness. The residue was dissolved in CH_3OH (500 mL) along with 1,3-bis(methoxycarbonyl)-2-methyl-2-thiopseudourea (32.1 g, 156 mmol) and acetic

acid (39 mL, 619 mmol) and stirred at rt for 1 h. A precipitate appeared and stirring was continued overnight. $NaOCH_3$ (73.1 g, 1353 mmol) was added. An exotherm was observed and the reaction mixture was stirred overnight. The reaction mixture was brought to pH 5 via addition of acetic acid and the precipitate was isolated by filtration, triturated with water (2 x 350 mL), CH_3CN (350 mL) and diisopropylether (350 mL).

Methyl (4-chloro-5*H*-pyrrolo[3,2-*d*]pyrimidin-2-yl)carbamate (11). Methyl *N*-(4-hydroxy-5*H*-pyrrolo[3,2-*d*]pyrimidin-2-yl)carbamate (25 g, 120 mmol) was dispensed into acetonitrile (350 mL) in a 500 mL multi neck flask at rt. $POCl_3$ (22.1 mL, 238.2 mmol) was added and the reaction mixture was heated to 70ºC while stirring by an overhead, mechanical stirrer at 300 rpm. *N,N*-diisopropylethylamine (41.4 mL, 240.2 mmol) was added drop-wise by a syringe pump at a flow rate of 0.2 mL/min. The reaction mixture was cooled to rt and poured into a stirred solution of sodium acetate (78.8 g, 961 mmol) in water (500 mL) at 45ºC. The organic solvents were removed under reduced pressure and the remaining liquid was stirred and cooled in an ice bath. The formed solid was isolated by filtration, washed with CH_3CN and triturated with diisopropylether to afford the titled compound as an off-white solid. ^{1}H NMR (400 MHz, DMSO-d_6) Shift 12.27 (br s, 1H), 10.22 (s, 1H), 7.92 (t, J=2.97 Hz, 1H), 6.57 (dd, J=1.76, 3.08 Hz, 1H), 3.66 (s, 3H).

Methyl (4-chloro-5-(pyridin-2-ylmethyl)-5*H*-pyrrolo[3,2-*d*]pyrimidin-2-yl)carbamate (**12**). To a suspension of methyl (4-chloro-5*H*-pyrrolo[3,2-*d*]pyrimidin-2-yl)carbamate. (5 g, 22 mmol), 2-pyridinemethanol (2.6 mL, 26.5 mmol) and polystyrene-bound triphenylphosphine (18.4 g, 55.2 mmol) in anhydrous THF (153 mL) was added DIAD (6.9 mL, 33 mmol) at rt and the reaction mixture stirred for 30 minutes, then was concentrated under reduced pressure. The product was purified via silica gel column chromatography using a gradient of CH_2Cl_2:CH_3OH

100:0 to 90:10. The product fractions were collected and concentrated under reduced pressure. The product was recrystallized in CH_3CN, isolated by filtration and dried under vacuum to afford the titled compound as a white solid.

4-chloro-5-(pyridin-2-ylmethyl)-5*H*-pyrrolo[3,2-*d*]pyrimidin-2-amine (13). Methyl (4-chloro-5-(pyridin-2-ylmethyl)-5*H*-pyrrolo[3,2-*d*]pyrimidin-2-yl)carbamate (4.5 g, 14.2 mmol) was dissolved in 1,4-dioxane (68 mL) in a 100 mL round bottom flask and NaOH (1 N aq., 34 mL) was added. The mixture was heated at 60°C for 5h. The mixture was cooled and concentrated under reduced pressure. The crude was treated with water and the precipitate was isolated by filtration and dried to afford the titled compound. The product was used without further purification in the next step.

N^4-butyl-5-(2-phenoxyethyl)-5*H*-pyrrolo[3,2-*d*]pyrimidine-2,4-diamine (14). ^{1}H NMR (360 MHz, DMSO-d_6) δ 7.20-7.28 (m, 3H), 6.92 (t, *J*=7.50 Hz, 1H), 6.82 (dd, *J*=0.73, 8.78 Hz, 2H), 6.32 (t, *J*=5.31 Hz, 1H), 5.94 (d, *J*=2.93 Hz, 1H), 5.36 (br s, 2H), 4.62 (t, *J*=5.31 Hz, 2H), 4.16 (t, *J*=5.12 Hz, 2H), 3.39-3.49 (m, 2H), 1.58 (quin, *J*=7.32 Hz, 2H), 1.35 (qd, *J*=7.38, 14.82 Hz, 2H), 0.89 (t, *J*=7.32 Hz, 3H).^{13}C NMR (91 MHz, DMSO-d_6) δ 156.7, 156.6, 149.3, 148.9, 131.2, 128.3, 119.7, 113.1, 108.9, 97.6, 66.7, 46.5, 38.4, 30.1, 18.6, 12.6. ESI-HRMS (TOF) *m/z*: 326.1980 (Calcd. for $C_{18}H_{23}N_5O$ $[M+H]^+$: 326.1980).

N^4-butyl-5-(3-phenylpropyl)-5*H*-pyrrolo[3,2-*d*]pyrimidine-2,4-diamine (15). ^{1}H NMR (400 MHz, DMSO-d_6) δ 7.22-7.30 (m, 2H), 7.08-7.22 (m, 4H), 6.34 (br t, *J*=5.50 Hz, 1H), 5.94 (d, *J*=3.08 Hz, 1H), 5.59 (br s, 2H), 4.29 (t, *J*=7.04 Hz, 2H), 3.38-3.51 (m, 2H), 2.39-2.55 (m, 2H), 1.82-1.99 (m, 2H), 1.49-1.64 (m, 2H), 1.34 (qd, *J*=7.40, 14.99 Hz, 2H), 0.90 (t, *J*=7.37 Hz, 3H).^{13}C NMR (101 MHz, DMSO-d_6) δ 157.6, 151.1, 148.8, 141.6, 132.8, 128.8, 128.5, 126.3, 109.9, 98.3, 48.7, 40.1, 33.8, 32.3, 31.8, 20.2, 14.3. ESI-HRMS (TOF) *m/z*: 324.2189 (Calcd. for $C_{19}H_{25}N_5$ $[M+H]^+$: 324.2188).

2-(2-amino-4-(butylamino)-5*H*-pyrrolo[3,2-*d*]pyrimidin-5-yl)-*N*-methylacetamide (16). ^{1}H NMR (400 MHz, DMSO-d_6) δ 8.32 (br d, *J*=4.40 Hz, 1H), 7.11 (d, *J*=3.08 Hz, 1H), 6.93 (t, *J*=5.17 Hz, 1H), 5.94 (d, *J*=2.86 Hz, 1H), 5.38 (br s, 2H), 4.74 (s, 2H), 3.31-3.45 (m, 2H), 2.64 (d, *J*=4.62 Hz, 3H), 1.49-1.64 (m, 2H), 1.29-1.44 (m, 2H), 0.92 (t, *J*=7.37 Hz, 3H).^{13}C NMR (101 MHz, DMSO-d_6) δ 169.4, 158.5, 151.4, 150.1, 132.7, 111.4, 99.5, 51.9, 31.6, 26.1, 20.2, 14.3. ESI-HRMS (TOF) *m/z*: 277.1779 (Calcd. for $C_{13}H_{20}N_6O$ $[M+H]^+$: 277.1777).

N^4-butyl-5-(3-methylbut-2-en-1-yl)-5*H*-pyrrolo[3,2-*d*]pyrimidine-2,4-diamine (17). ^{1}H NMR (360 MHz, DMSO-d_6) δ 7.14 (d, *J*=2.93 Hz, 1H), 5.98 (t, *J*=5.49 Hz, 1H), 5.89 (d, *J*=2.93 Hz,

1H), 5.41 (br s, 2H), 5.21 (ddd, *J*=1.46, 5.21, 6.50 Hz, 1H), 4.83 (br d, *J*=6.59 Hz, 2H), 3.34-3.47 (m, 2H), 1.73 (s, 3H), 1.69 (s, 3H), 1.48-1.61 (m, 2H), 1.34 (qd, *J*=7.35, 14.91 Hz, 2H), 0.87-0.96 (m, 3H).^{13}C NMR (91 MHz, DMSO-d_6) δ 156.5, 149.4, 148.5, 134.0, 130.2, 120.2, 108.7, 97.1, 45.4, 38.3, 30.0, 24.0, 18.4, 16.6, 12.6. ESI-HRMS (TOF) *m/z*: 274.2034 (Calcd. for $C_{15}H_{23}N_5$ $[M+H]^+$: 274.2031)

N^4-butyl-5-(thiophen-3-ylmethyl)-5*H*-pyrrolo[3,2-*d*]pyrimidine-2,4-diamine Hydrochloride (18). ^{1}H NMR (400 MHz, DMSO-d_6) δ 12.68 (br s, 1H), 7.55-7.67 (m, 2H), 7.50 (dd, *J*=2.86, 4.84 Hz, 1H), 7.37 (br s, 2H), 7.25 (br s, 1H), 6.82 (d, *J*=4.84 Hz, 1H), 6.22 (d, *J*=2.86 Hz, 1H), 5.70 (s, 2H), 3.48 (q, *J*=6.53 Hz, 2H), 1.44 (quin, *J*=7.15 Hz, 2H), 1.11 (qd, *J*=7.29, 14.88 Hz, 2H), 0.75-0.90 (m, 3H).^{13}C NMR (101 MHz, DMSO-d_6) δ 153.1, 151.9, 138.8, 136.7, 134.8, 127.7, 126.7, 122.8, 108.5, 95.4, 48.0, 40.4, 31.1, 19.7, 14.2. ESI-HRMS (TOF) *m/z*: 302.1442 (Calcd. for $C_{15}H_{19}N_5S$ $[M+H]^+$: 302.1439).

N^4-butyl-5-(thiazol-2-ylmethyl)-5*H*-pyrrolo[3,2-*d*]pyrimidine-2,4-diamine (19). ^{1}H NMR (360 MHz, DMSO-d_6) δ 7.77 (d, *J*=3.29 Hz, 1H), 7.67 (d, *J*=3.29 Hz, 1H), 7.36 (d, *J*=2.93 Hz, 1H), 6.50 (t, *J*=5.31 Hz, 1H), 5.99 (d, *J*=3.29 Hz, 1H), 5.80 (s, 2H), 5.33 (s, 2H), 3.28-3.40 (m, 2H), 1.49 (quin, *J*=7.23 Hz, 2H), 1.24 (qd, *J*=7.49, 14.87 Hz, 2H), 0.86 (t, *J*=7.32 Hz, 3H).^{13}C NMR (91 MHz, DMSO-d_6) δ 166.6, 157.2, 150.0, 149.2, 141.0, 130.9, 120.2, 108.8, 98.9, 47.7, 38.3, 29.8, 18.3, 12.6. ESI-HRMS (TOF) *m/z*: 303.1393 (Calcd. for $C_{14}H_{18}N_6S$ $[M+H]^+$: 303.1392)

N^4-butyl-5-(imidazo[1,2-*a*]pyridin-2-ylmethyl)-5*H*-pyrrolo[3,2-*d*]pyrimidine-2,4-diamine (20). ^{1}H NMR (400 MHz, DMSO-d_6) δ 8.49-8.60 (m, 1H), 7.83-7.92 (m, 2H), 7.50 (dd, *J*=0.66, 9.02 Hz, 1H), 7.39 (d, *J*=2.86 Hz, 1H), 7.29 (ddd, *J*=1.10, 6.71, 9.13 Hz, 1H), 6.92 (dt, *J*=1.10,

6.71 Hz, 1H), 5.97 (d, *J*=2.86 Hz, 1H), 5.69 (br s, 2H), 5.49 (s, 2H), 3.41-3.50 (m, 2H), 1.60 (quin, *J*=7.26 Hz, 2H), 1.31 (qd, *J*=7.40, 14.99 Hz, 2H), 0.86 (t, *J*=7.37 Hz, 3H).^{13}C NMR (101 MHz, DMSO-d_6) δ 157.3, 151.6, 144.5, 143.2, 132.6, 127.8, 126.2, 116.7, 113.0, 111.4, 110.7, 98.4, 46.5, 40.5, 31.4, 20.2, 14.2. ESI-HRMS (TOF) *m/z*: 336.1941 (Calcd. for $C_{18}H_{21}N_7$ $[M+H]^+$: 336.1937).

N^4-butyl-5-(pyridin-2-ylmethyl)-5*H*-pyrrolo[3,2-*d*]pyrimidine-2,4-diamine (21). ^{1}H NMR (360 MHz, DMSO-d_6) δ 8.54 (d, *J*=4.76 Hz, 1H), 8.07 (br t, *J*=5.12 Hz, 1H), 7.85 (dt, *J*=1.46, 7.68 Hz, 1H), 7.57 (d, *J*=2.93 Hz, 1H), 7.38 (dd, *J*=5.12, 7.32 Hz, 1H), 7.34 (d, *J*=7.68 Hz, 1H), 6.56 (br s, 2H), 6.11 (d, *J*=2.93 Hz, 1H), 5.57 (s, 2H), 3.40-3.51 (m, 2H), 1.54 (quin, *J*=7.23 Hz, 2H), 1.15-1.31 (m, 2H), 0.87 (t, *J*=7.32 Hz, 3H).^{13}C NMR (91 MHz, DMSO-d_6) δ 156.8, 156.2, 149.6, 148.7, 147.5, 136.7, 130.8, 122.1, 121.7, 121.1, 109.1, 97.9, 52.2, 29.8, 18.4, 12.6. ESI-HRMS (TOF) *m/z*: 297.1833 (Calcd. for $C_{16}H_{20}N_6$ $[M+H]^+$: 297.1828).

N^4-butyl-5-(pyridin-3-ylmethyl)-5*H*-pyrrolo[3,2-*d*]pyrimidine-2,4-diamine (22). ^{1}H NMR (360 MHz, DMSO-d_6) δ 8.44 (dd, *J*=1.46, 4.76 Hz, 1H), 8.25 (d, *J*=1.83 Hz, 1H), 7.49 (d, *J*=2.93 Hz, 1H), 7.27-7.36 (m, 1H), 7.22-7.27 (m, 1H), 6.75 (t, *J*=5.27 Hz, 1H), 6.21 (br s, 2H), 6.12 (d, *J*=2.93 Hz, 1H), 5.65 (s, 2H), 3.33-3.40 (m, 2H), 1.28-1.42 (m, 2H), 0.91-1.06 (m, 2H), 0.71-0.80 (m, 3H).^{13}C NMR (91 MHz, DMSO-d_6) δ 154.8, 150.2, 147.5, 149.8, 146.4, 132.8, 132.6, 132.5, 122.5, 107.9, 96.8, 48.0, 39.3, 29.8, 18.1, 12.6. ESI-HRMS (TOF) *m/z*: 297.1833 (Calcd. for $C_{16}H_{20}N_6$ $[M+H]^+$: 297.1828).

N^4-butyl-5-(pyridin-4-ylmethyl)-5*H*-pyrrolo[3,2-*d*]pyrimidine-2,4-diamine (23). ^{1}H NMR (400 MHz, DMSO-d_6) δ 8.46 (d, *J*=5.16 Hz, 2H), 7.39 (d, *J*=3.08 Hz, 1H), 6.83 (d, *J*=5.94 Hz, 2H), 6.19 (br s, 1H), 6.08 (d, *J*=2.86 Hz, 1H), 5.66-5.75 (m, 2H), 5.60 (s, 2H), 3.17 (br. s., 2H),

1.32 (td, *J*=7.54, 14.86 Hz, 2H), 0.97 (sxt, *J*=7.39 Hz, 2H), 0.69-0.79 (m, 3H).^{13}C NMR (101 MHz, DMSO-d_6) δ 157.7, 151.1, 150.2, 148.3, 133.8, 121.3, 110.0, 99.3, 50.9, 40.9, 31.4, 19.7, 14.1. ESI-HRMS (TOF) *m/z*: 297.1835 (Calcd. for $C_{16}H_{20}N_6$ $[M+H]^+$: 297.1828).

N^4-butyl-5-((6-methylpyridin-2-yl)methyl)-5*H*-pyrrolo[3,2-*d*]pyrimidine-2,4-diamine (24). ^{1}H NMR (400 MHz, DMSO-d_6) δ 7.59-7.83 (m, 2H), 7.46 (br d, *J*=2.20 Hz, 1H), 7.23 (br d, *J*=7.48 Hz, 1H), 7.07 (br d, *J*=7.48 Hz, 1H), 6.02 (br d, *J*=2.42 Hz, 1H), 5.81 (br s, 2H), 5.44 (s, 2H), 3.44 (br d, *J*=5.50 Hz, 2H), 2.49 (s, 3H), 1.47-1.69 (m, 2H), 1.17-1.39 (m, 2H), 0.89 (br t, *J*=7.26 Hz, 3H).^{13}C NMR (101 MHz, DMSO-d_6) δ 157.8, 157.2, 156.9, 151.6, 147.2, 138.8, 132.8, 123.2, 120.0, 110.4, 98.7, 53.8, 31.6, 24.2, 20.1, 14.2. ESI-HRMS (TOF) *m/z*: 311.1988 $[M+H]^+$ (Calcd. for $C_{17}H_{22}N_6$: 310.1906). ESI-HRMS (TOF) *m/z*: 311.1988 (Calcd. for $C_{17}H_{22}N_6$ $[M+H]^+$: 311.1984).

N^4-butyl-5-(quinolin-2-ylmethyl)-5*H*-pyrrolo[3,2-*d*]pyrimidine-2,4-diamine (25). ^{1}H NMR (360 MHz, DMSO-d_6) δ 8.39 (d, *J*=8.42 Hz, 1H), 7.95-8.02 (m, 2H), 7.83 (ddd, *J*=1.46, 6.95, 8.42 Hz, 1H), 7.63 (t, *J*=7.39 Hz, 1H), 7.56 (d, *J*=3.20 Hz, 1H), 7.26 (d, *J*=8.42 Hz, 1H), 7.02 (t, *J*=5.31 Hz, 1H), 6.05 (d, *J*=2.93 Hz, 1H), 5.70 (s, 2H), 5.53 (br s, 2H), 3.32-3.45 (m, 2H), 1.38-1.48 (m, 2H), 1.11 (qd, *J*=7.46, 14.96 Hz, 2H), 0.71 (t, *J*=7.32 Hz, 3H).^{13}C NMR (91 MHz, DMSO-d_6) δ 157.1, 156.5, 149.4, 148.0, 145.2, 136.8, 131.1, 129.0, 126.9, 126.8, 125.9, 125.6, 118.6, 108.9, 97.8, 53.0, 38.3, 29.9, 18.3, 12.4. ESI-HRMS (TOF) *m/z*: 347.1983 (Calcd. for $C_{20}H_{22}N_6$ $[M+H]^+$: 347.1984).

N^4-butyl-5-((4-methoxy-3,5-dimethylpyridin-2-yl)methyl)-5*H*-pyrrolo[3,2-*d*]pyrimidine-2,4-diamine (26). ^{1}H NMR (400 MHz, DMSO-d_6) δ 8.21 (s, 1H), 7.86 (t, *J*=4.95 Hz, 1H), 7.30 (d, *J*=3.08 Hz, 1H), 5.92 (d, *J*=2.86 Hz, 1H), 5.44 (s, 2H), 5.23 (s, 2H), 3.71 (s, 3H), 3.39 (dt,

J=5.28, 6.93 Hz, 2H), 2.32 (s, 3H), 2.21 (s, 3H), 1.53-1.69 (m, 2H), 1.37 (qd, *J*=7.38, 14.83 Hz, 2H), 0.93 (t, *J*=7.37 Hz, 3H).^{13}C NMR (101 MHz, DMSO-d_6) δ 164.8, 158.6, 155.3, 151.2, 150.6, 148.7, 132.6, 126.8, 126.0, 111.3, 99.3, 60.3, 52.1, 40.3, 31.5, 20.3, 14.3, 13.4, 11.1. ESI-HRMS (TOF) *m/z*: 355.2244 (Calcd. for $C_{19}H_{26}N_6O$ $[M+H]^+$: 355.2246).

N^4-butyl-5-((3-methoxypyridin-2-yl)methyl)-5*H*-pyrrolo[3,2-*d*]pyrimidine-2,4-diamine (27). ^{1}H NMR (360 MHz, DMSO-d_6) δ 8.10 (dd, *J*=1.46, 4.76 Hz, 1H), 7.61 (t, *J*=4.94 Hz, 1H), 7.54 (dd, *J*=1.10, 8.42 Hz, 1H), 7.42 (dd, *J*=4.76, 8.42 Hz, 1H), 7.21 (d, *J*=2.93 Hz, 1H), 5.90 (d, *J*=2.93 Hz, 1H), 5.38 (s, 2H), 5.24 (s, 2H), 3.90 (s, 3H), 3.42 (dt, *J*=5.12, 6.95 Hz, 2H), 1.59-1.68 (m, 2H), 1.41 (qd, *J*=7.30, 15.05 Hz, 2H), 0.91-0.97 (m, 3H).^{13}C NMR (91 MHz, DMSO-d_6) δ 156.9, 152.7, 149.3, 148.9, 144.4, 138.4, 131.2, 123.9, 118.4, 109.3, 97.5, 54.6, 47.6, 38.7, 29.8, 18.6, 12.6. ESI-HRMS (TOF) *m/z*: 327.1934 (Calcd. for $C_{17}H_{22}N_6O$ $[M+H]^+$: 327.1933).

N^4-(2-methoxyethyl)-5-(pyridin-2-ylmethyl)-5*H*-pyrrolo[3,2-*d*]pyrimidine-2,4-diamine (28). ^{1}H NMR (360 MHz, DMSO-d_6) δ 8.55 (dd, *J*=0.73, 4.03 Hz, 1H), 7.82 (dt, *J*=1.83, 7.68 Hz, 1H), 7.43 (t, *J*=5.31 Hz, 1H), 7.40 (d, *J*=3.29 Hz, 1H), 7.35 (dd, *J*=5.12, 7.32 Hz, 1H), 7.29 (d, *J*=8.05 Hz, 1H), 5.96 (d, *J*=2.93 Hz, 1H), 5.44 (s, 2H), 5.39 (br s, 2H), 3.56 (q, *J*=5.37 Hz, 2H), 3.41-3.52 (m, 2H), 3.24 (s, 3H).^{13}C NMR (91 MHz, DMSO-d_6) δ 156.9, 156.0, 149.5, 147.7, 149.2, 136.8, 130.9, 122.1, 121.2, 109.2, 98.0, 69.5, 56.8, 52.2, 38.5. ESI-HRMS (TOF) *m/z*: 299.1624 (Calcd. for $C_{15}H_{18}N_6O$ $[M+H]^+$: 299.1620).

N^4-(3-methoxypropyl)-5-(pyridin-2-ylmethyl)-5*H*-pyrrolo[3,2-*d*]pyrimidine-2,4-diamine (29). ^{1}H NMR (360 MHz, DMSO-d_6) δ 8.55 (d, *J*=4.76 Hz, 1H), 7.81 (dt, *J*=1.46, 7.68 Hz, 1H), 7.38 (d, *J*=3.26 Hz, 1H), 7.32-7.37 (m, 1H), 7.15 (d, *J*=7.87 Hz, 1H), 7.05 (t, *J*=5.14 Hz, 1H), 5.97 (d, *J*=2.93 Hz, 1H), 5.48 (s, 2H), 5.30 (s, 2H), 3.39-3.43 (m, 2H), 3.31 (t, *J*=6.40 Hz, 2H),

3.19 (s, 3H), 1.78 (quin, *J*=6.59 Hz, 2H).^{13}C NMR (91 MHz, DMSO-d_6) δ 157.1, 156.4, 149.6, 149.5, 147.6, 136.7, 130.9, 122.0, 121.0, 109.2, 98.2, 68.7, 56.7, 52.2, 36.2, 27.8. ESI-HRMS (TOF) *m/z*: 313.1780 (Calcd. for $C_{16}H_{20}N_6O$ $[M+H]^+$: 313.1777).

N^4-(2-ethoxyethyl)-5-(pyridin-2-ylmethyl)-5*H*-pyrrolo[3,2-*d*]pyrimidine-2,4-diamine (30). ^{1}H NMR (360 MHz, DMSO-d_6) δ 8.55 (d, *J*=5.12 Hz, 1H), 7.81 (dt, *J*=1.83, 7.68 Hz, 1H), 7.39 (d, *J*=2.93 Hz, 1H), 7.34 (dt, *J*=5.12, 7.14 Hz, 2H), 7.25 (d, *J*=7.68 Hz, 1H), 5.96 (d, *J*=2.93 Hz, 1H), 5.44 (s, 2H), 5.33 (s, 2H), 3.52-3.58 (m, 2H), 3.47-3.52 (m, 2H), 3.42 (q, *J*=7.07 Hz, 2H), 1.07 (t, *J*=6.95 Hz, 3H).^{13}C NMR (91 MHz, DMSO-d_6) δ 157.1, 156.2, 149.6, 149.5, 147.7, 136.8, 130.9, 122.1, 121.2, 109.3, 98.2, 67.4, 64.3, 52.2, 46.8, 14.0. ESI-HRMS (TOF) *m/z*: 313.1781 (Calcd. for $C_{16}H_{20}N_6O$ $[M+H]^+$: 313.1777).

1-((2-amino-5-(pyridin-2-ylmethyl)-5*H*-pyrrolo[3,2-*d*]pyrimidin-4-yl)amino)butan-2-ol (31). ^{1}H NMR (360 MHz, DMSO-d_6) δ 8.54 (d, *J*=4.76 Hz, 1H), 7.81 (dt, *J*=1.83, 7.68 Hz, 1H), 7.39 (d, *J*=2.93 Hz, 1H), 7.34 (dd, *J*=4.94, 6.77 Hz, 1H), 7.18-7.27 (m, 2H), 5.96 (d, *J*=2.93 Hz, 1H), 5.47 (s, 2H), 5.30 (s, 2H), 4.84 (br s, 1H), 3.54 (quin, *J*=5.85 Hz, 1H), 3.41-3.50 (m, 1H), 3.24-3.34 (m, 1H), 1.21-1.43 (m, 2H), 0.86 (t, *J*=7.32 Hz, 3H).^{13}C NMR (91 MHz, DMSO-d_6) δ 156.9, 156.1, 149.6, 149.5, 147.7, 147.7, 136.6, 130.9, 121.9, 121.0, 98.1, 69.4, 52.1, 44.9, 26.2, 8.8. ESI-HRMS (TOF) *m/z*: 313.1699 (Calcd. for $C_{16}H_{20}N_6O$ $[M+H]^+$: 313.1777).

N^4-((5-methylpyridin-2-yl)methyl)-5-(pyridin-2-ylmethyl)-5*H*-pyrrolo[3,2-*d*]pyrimidine-2,4-diamine (32). ^{1}H NMR (360 MHz, DMSO-d_6) δ 8.43 (d, *J*=4.89 Hz, 1H), 8.32 (s, 1H), 7.79 (dt, *J*=1.83, 7.68 Hz, 1H), 7.65 (t, *J*=5.67 Hz, 1H), 7.38-7.47 (m, 2H), 7.32 (dd, *J*=4.94, 6.77 Hz, 1H), 7.12 (d, *J*=8.05 Hz, 1H), 6.95 (d, *J*=8.05 Hz, 1H), 6.00 (d, *J*=2.93 Hz, 1H), 5.55 (s, 2H), 5.31 (s, 2H), 4.68 (d, *J*=5.49 Hz, 2H), 2.25 (s, 3H).^{13}C NMR (91 MHz, DMSO-d_6) δ 157.2,

156.5, 155.4, 150.1, 149.3, 147.8, 142.5, 136.7, 135.7, 131.4, 129.6, 122.0, 120.8, 119.3, 109.4, 98.4, 52.3, 43.7, 16.5. ESI-HRMS (TOF) *m/z*: 346.1785 (Calcd. for $C_{19}H_{19}N_7$ $[M+H]^+$: 346.1780).

N^4-(1-(pyridin-2-yl)ethyl)-5-(pyridin-2-ylmethyl)-5*H*-pyrrolo[3,2-*d*]pyrimidine-2,4-diamine (33). ^{1}H NMR (360 MHz, DMSO-d_6) δ 8.46-8.51 (m, 2H), 7.84 (t, *J*=7.56 Hz, 1H), 7.80 (d, *J*=7.41 Hz, 1H), 7.66 (dt, *J*=1.83, 7.68 Hz, 1H), 7.45 (d, *J*=2.93 Hz, 1H), 7.25-7.38 (m, 3H), 7.21 (dd, *J*=5.12, 7.32 Hz, 1H), 5.96 (d, *J*=2.93 Hz, 1H), 5.47-5.58 (m, 2H), 5.42 (t, *J*=6.95 Hz, 1H), 5.24 (s, 2H), 1.52 (d, *J*=6.95 Hz, 3H).^{13}C NMR (91 MHz, DMSO-d_6) δ 161.9, 156.8, 155.9, 148.4, 147.4, 141.0, 136.7, 136.6, 135.2, 124.8, 122.0, 121.0, 119.7, 119.1, 115.0, 97.9, 52.2, 48.7, 20.2. ESI-HRMS (TOF) *m/z*: 346.1780 (Calcd. for $C_{19}H_{19}N_7$ $[M+H]^+$: 346.1780).

N^4-((2-methylthiazol-4-yl)methyl)-5-(pyridin-2-ylmethyl)-5*H*-pyrrolo[3,2-*d*]pyrimidine-2,4-diamine (34). ^{1}H NMR (360 MHz, DMSO-d_6) δ 8.44 (d, *J*=4.87 Hz, 1H), 7.75-7.85 (m, 2H), 7.41 (d, *J*=2.93 Hz, 1H), 7.33 (dd, *J*=4.94, 7.50 Hz, 1H), 7.23 (d, *J*=7.32 Hz, 1H), 7.01 (s, 1H), 5.98 (d, *J*=2.20 Hz, 1H), 5.49 (s, 2H), 5.36 (s, 2H), 4.67 (d, *J*=5.49 Hz, 2H), 2.63 (s, 3H).^{13}C NMR (91 MHz, DMSO-d_6) δ 163.9, 157.1, 156.3, 153.4, 150.0, 149.2, 147.7, 136.9, 131.2, 122.1, 121.3, 113.1, 109.4, 98.3, 52.2, 17.7. ESI-HRMS (TOF) *m/z*: 352.1353 (Calcd. for $C_{17}H_{17}N_7S$ $[M+H]^+$: 352.1344).

N^4-((5-methyl-1,3,4-oxadiazol-2-yl)methyl)-5-(pyridin-2-ylmethyl)-5*H*-pyrrolo[3,2-*d*]pyrimidine-2,4-diamine (35). ^{1}H NMR (360 MHz, DMSO-d_6) δ 8.45 (d, *J*=4.76 Hz, 1H), 8.05 (t, *J*=5.67 Hz, 1H), 7.80 (dt, *J*=1.83, 7.68 Hz, 1H), 7.44 (d, *J*=2.93 Hz, 1H), 7.34 (dd, *J*=5.12, 6.95 Hz, 1H), 7.23 (d, *J*=8.05 Hz, 1H), 5.99 (d, *J*=2.93 Hz, 1H), 5.49 (s, 2H), 5.37 (s, 2H), 4.85 (d, *J*=5.85 Hz, 2H), 2.43 (s, 3H).^{13}C NMR (91 MHz, DMSO-d_6) δ 163.5, 162.3, 156.7, 156.0,

150.3, 148.5, 147.5, 136.7, 131.6, 122.0, 121.1, 109.2, 98.2, 52.0, 33.3, 9.2. ESI-HRMS (TOF) *m/z*: 337.1525 (Calcd. for $C_{16}H_{16}N_8O$ $[M+H]^+$: 337.1525).

***N*^{4}-(oxazol-2-ylmethyl)-5-(pyridin-2-ylmethyl)-5*H*-pyrrolo[3,2-*d*]pyrimidine-2,4-diamine (36).** ^{1}H NMR (360 MHz, DMSO-d_6) δ 8.42 (d, *J*=4.89 Hz, 1H), 8.08 (t, *J*=5.67 Hz, 1H), 8.00 (s, 1H), 7.81 (dt, *J*=1.83, 7.68 Hz, 1H), 7.43 (d, *J*=2.93 Hz, 1H), 7.28-7.36 (m, 2H), 7.14 (s, 1H), 5.98 (d, *J*=2.93 Hz, 1H), 5.47 (s, 2H), 5.35 (s, 2H), 4.79 (d, *J*=5.49 Hz, 2H).^{13}C NMR (91 MHz, DMSO-d_6) δ 160.8, 156.8, 155.9, 150.1, 148.8, 147.5, 138.3, 136.7, 131.4, 125.7, 122.0, 121.3, 109.3, 98.2, 52.0, 35.7. ESI-HRMS (TOF) *m/z*: 322.1426 (Calcd. for $C_{16}H_{15}N_7O$ $[M+H]^+$: 322.1416).

***N*^{4}-((5-methyloxazol-2-yl)methyl)-5-(pyridin-2-ylmethyl)-5*H*-pyrrolo[3,2-*d*]pyrimidine-2,4-diamine (37).** ^{1}H NMR (360 MHz, DMSO-d_6) δ 8.42 (d, *J*=3.66 Hz, 1H), 8.01 (t, *J*=5.67 Hz, 1H), 7.81 (t, *J*=7.43 Hz, 1H), 7.43 (d, *J*=2.93 Hz, 1H), 7.25-7.36 (m, 2H), 6.74 (s, 1H), 5.98 (d, *J*=2.93 Hz, 1H), 5.47 (s, 2H), 5.34 (s, 2H), 4.72 (d, *J*=5.49 Hz, 2H), 2.23 (s, 3H). ^{13}C NMR (101 MHz, DMSO-d_6) δ 161.1, 158.5, 157.6, 151.7, 150.5, 149.2, 148.9, 138.4, 133.0, 123.7, 123.0, 111.0, 99.9, 53.7, 37.4, 11.0. ESI-HRMS (TOF) *m/z*: 336.1575 (Calcd. for $C_{17}H_{17}N_7O$ $[M+H]^+$: 336.1572).

***N*^{4}-((4-methyloxazol-2-yl)methyl)-5-(pyridin-2-ylmethyl)-5*H*-pyrrolo[3,2-*d*]pyrimidine-2,4-diamine (38).** ^{1}H NMR (360 MHz, DMSO-d_6) δ 8.43 (d, *J*=4.76 Hz, 1H), 8.03 (t, *J*=5.49 Hz, 1H), 7.80 (dt, *J*=1.83, 7.68 Hz, 1H), 7.67 (d, *J*=1.46 Hz, 1H), 7.43 (d, *J*=2.93 Hz, 1H), 7.27-7.36 (m, 2H), 5.98 (d, *J*=2.93 Hz, 1H), 5.47 (s, 2H), 5.35 (s, 2H), 4.73 (d, *J*=5.49 Hz, 2H), 2.05 (d, *J*=1.10 Hz, 3H).^{13}C NMR (101 MHz, DMSO-d_6) δ 162.0, 158.5, 157.6, 151.8, 150.5, 149.2,

138.4, 136.1, 135.2, 133.1, 123.6, 123.0, 111.0, 99.9, 53.8, 37.4, 11.7. ESI-HRMS (TOF) *m/z*: 336.1573 (Calcd. for $C_{17}H_{17}N_7O$ $[M+H]^+$: 336.1572).

5-(pyridin-2-ylmethyl)-*N*^{4}-(thiazol-2-ylmethyl)-5*H*-pyrrolo[3,2-*d*]pyrimidine-2,4-diamine (39). ^{1}H NMR (360 MHz, DMSO-d_6) δ 8.44 (d, *J*=4.76 Hz, 1H), 8.12 (t, *J*=5.85 Hz, 1H), 7.78 (t, *J*=7.73 Hz, 1H), 7.71 (d, *J*=3.21 Hz, 1H), 7.52 (d, *J*=3.29 Hz, 1H), 7.43 (d, *J*=3.29 Hz, 1H), 7.31 (dd, *J*=4.94, 6.77 Hz, 1H), 7.14 (d, *J*=7.68 Hz, 1H), 6.01 (d, *J*=2.93 Hz, 1H), 5.53 (s, 2H), 5.41 (s, 2H), 4.94 (d, *J*=5.49 Hz, 2H). ^{13}C NMR (91 MHz, DMSO-d_6) δ 169.7, 156.9, 156.3, 150.4, 147.7, 148.7, 141.0, 136.7, 131.8, 122.0, 120.9, 118.6, 109.3, 98.4, 52.1, 40.3. ESI-HRMS (TOF) *m/z*: 338.1191 (Calcd. for $C_{16}H_{15}N_7S$ $[M+H]^+$: 338.1188).

***N*^{4}-((5-methylthiazol-2-yl)methyl)-5-(pyridin-2-ylmethyl)-5*H*-pyrrolo[3,2-*d*]pyrimidine-2,4-diamine (40).** ^{1}H NMR (360 MHz, DMSO-d_6) δ 13.09 (br s, 1H), 9.40 (br s, 1H), 8.65 (br d, *J*=5.12 Hz, 1H), 8.10 (t, *J*=7.32 Hz, 1H), 7.55-7.79 (m, 4H), 7.47 (s, 1H), 7.32 (d, *J*=7.68 Hz, 1H), 6.34 (d, *J*=2.56 Hz, 2H), 4.95 (br d, *J*=4.39 Hz, 2H), 2.36 (s, 3H).^{13}C NMR (91 MHz, DMSO-d_6) δ 165.6, 153.1, 151.4, 150.2, 145.0, 140.5, 137.3, 135.7, 134.3, 133.2, 123.3, 122.0, 107.6, 94.7, 50.1, 40.3, 10.3. ESI-HRMS (TOF) *m/z*: 352.1348 (Calcd. for $C_{17}H_{17}N_7S$ $[M+H]^+$: 352.1344).

***N*^{4}-(isoxazol-3-ylmethyl)-5-(pyridin-2-ylmethyl)-5*H*-pyrrolo[3,2-*d*]pyrimidine-2,4-diamine (41). 13** (175 mg, 0.67 mmol), isoxazol-3-yl-methylamine hydrochloride (136 mg, 1.0 mmol), and DIPEA (173 mg, 1.3 mmol) were dissolved in NMP (2.4 mL) in a 7 mL glass vial. The mixture was stirred at 100°C for 2h then cooled to rt and concentrated *in vacuo*. It was purified by Prep HPLC (Stationary phase: RP Vydac Denali C18 - 10 μm, 200 g, 5 cm), Mobile phase: 0.25% NH_4OAc solution in water, CH_3OH), the desired fractions were collected and

concentrated *in vacuo*. The product was triturated in CH_3CN, isolated by filtration and dried under vacuum to afford the titled compound as a white solid. ^{1}H NMR (360 MHz, DMSO-d_6) δ 8.78 (d, *J*=1.46 Hz, 1H), 8.41 (d, *J*=4.91 Hz, 1H), 7.90 (t, *J*=5.50 Hz, 1H), 7.79 (t, *J*=7.55 Hz, 1H), 7.41 (d, *J*=2.93 Hz, 1H), 7.31 (dd, *J*=4.94, 7.50 Hz, 1H), 7.19 (d, *J*=7.68 Hz, 1H), 6.38 (d, *J*=1.46 Hz, 1H), 5.99 (d, *J*=2.93 Hz, 1H), 5.48 (s, 2H), 5.41 (s, 2H), 4.70 (d, *J*=5.85 Hz, 2H).^{13}C NMR (91 MHz, DMSO-d_6) δ 160.7, 158.4, 157.0, 156.3, 150.2, 149.1, 147.6, 136.8, 131.5, 122.1, 121.2, 109.4, 103.4, 98.4, 52.2, 34.1. ESI-HRMS (TOF) *m/z*: 322.1422 (Calcd. for $C_{16}H_{15}N_7O$ $[M+H]^+$: 322.1416).

N^4-((5-methylisoxazol-3-yl)methyl)-5-(pyridin-2-ylmethyl)-5*H*-pyrrolo[3,2-*d*]pyrimidine-2,4-diamine (42). ^{1}H NMR (360 MHz, DMSO-d_6) δ 8.41 (br d, *J*=4.39 Hz, 1H), 8.17 (br s, 1H), 7.80 (br t, *J*=7.14 Hz, 1H), 7.48 (d, *J*=2.56 Hz, 1H), 7.28-7.38 (m, 1H), 7.21 (br d, *J*=7.68 Hz, 1H), 6.06 (d, *J*=2.56 Hz, 1H), 5.96 (s, 1H), 5.89 (br s, 2H), 5.52 (s, 2H), 4.65 (br d, *J*=4.76 Hz, 2H), 2.33 (s, 3H).^{13}C NMR (91 MHz, DMSO-d_6) δ 167.9, 161.4, 155.9, 155.7, 149.4, 147.6, 146.8, 136.8, 132.0, 122.1, 121.2, 109.0, 100.3, 97.4, 52.0, 34.2, 10.6. ESI-HRMS (TOF) *m/z*: 336.1575 (Calcd. for $C_{17}H_{17}N_7O$ $[M+H]^+$: 336.1572).

N^4-((5-cyclopropylisoxazol-3-yl)methyl)-5-(pyridin-2-ylmethyl)-5*H*-pyrrolo[3,2-*d*]pyrimidine-2,4-diamine (43). ^{1}H NMR (360 MHz, DMSO-d_6) δ 8.42 (d, *J*=4.76 Hz, 1H), 7.74-7.82 (m, 2H), 7.41 (d, *J*=2.85 Hz, 1H), 7.33 (t, *J*=5.99 Hz, 1H), 7.15 (d, *J*=7.68 Hz, 1H), 5.99 (d, *J*=2.93 Hz, 1H), 5.89 (s, 1H), 5.49 (s, 2H), 5.41 (s, 2H), 4.59 (d, *J*=5.85 Hz, 2H), 2.00-2.12 (m, 1H), 0.96-1.06 (m, 2H), 0.75-0.84 (m, 2H).^{13}C NMR (91 MHz, DMSO-d_6) δ 172.7, 161.5, 156.8, 156.1, 150.0, 148.8, 147.4, 147.4, 136.6, 131.3, 121.8, 120.9, 109.1, 98.2, 97.3, 51.9, 33.9, 6.8, 6.3. ESI-HRMS (TOF) *m/z*: 362.1729 (Calcd. for $C_{19}H_{19}N_7O$ $[M+H]^+$: 362.1729).

N^4-((5-isopropylisoxazol-3-yl)methyl)-5-(pyridin-2-ylmethyl)-5*H*-pyrrolo[3,2-*d*]pyrimidine-2,4-diamine (44). ^{1}H NMR (360 MHz, DMSO-d_6) δ 8.38-8.42 (m, 1H), 7.73-7.82 (m, 2H), 7.42 (d, *J*=3.20 Hz, 1H), 7.31 (t, *J*=5.90 Hz, 1H), 7.14 (d, *J*=8.05 Hz, 1H), 5.99 (d, *J*=2.93 Hz, 1H), 5.93 (s, 1H), 5.50 (s, 2H), 5.42 (s, 2H), 4.63 (d, *J*=5.49 Hz, 2H), 3.01 (spt, *J*=6.95 Hz, 1H), 1.18 (d, *J*=6.95 Hz, 6H).^{13}C NMR (101 MHz, DMSO-d_6) δ 178.2, 163.0, 158.6, 157.9, 151.8, 150.6, 149.1, 138.3, 133.1, 123.6, 122.6, 110.9, 100.0, 99.3, 53.7, 35.7, 26.9, 21.1. ESI-HRMS (TOF) *m/z*: 364.1891 (Calcd. for $C_{19}H_{21}N_7O$ $[M+H]^+$: 364.1886).

N^4-((3-methylisoxazol-5-yl)methyl)-5-(pyridin-2-ylmethyl)-5*H*-pyrrolo[3,2-*d*]pyrimidine-2,4-diamine (45). ^{1}H NMR (400 MHz, DMSO-d_6) δ 8.47 (d, *J*=5.01 Hz, 1H), 7.89 (t, *J*=5.67 Hz, 1H), 7.80 (t, *J*=7.71 Hz, 1H), 7.42 (d, *J*=3.11 Hz, 1H), 7.34 (t, *J*=6.19 Hz, 1H), 7.19 (d, *J*=7.92 Hz, 1H), 6.00 (d, *J*=3.08 Hz, 1H), 5.95 (s, 1H), 5.50 (s, 2H), 5.37 (s, 2H), 4.71 (d, *J*=5.50 Hz, 2H), 2.16 (s, 3H).^{13}C NMR (101 MHz, DMSO-d_6) δ 171.4, 159.8, 158.5, 157.9, 151.9, 149.3, 150.3, 138.4, 133.2, 123.7, 122.7, 111.0, 103.0, 100.0, 53.7, 36.1, 11.4. ESI-HRMS (TOF) *m/z*: 336.1577 (Calcd. for $C_{17}H_{17}N_7O$ $[M+H]^+$: 336.1572).

5-((5,6-dimethoxypyridin-2-yl)methyl)-N^4-((5-methylisoxazol-3-yl)methyl)-5*H*-pyrrolo[3,2-*d*]pyrimidine-2,4-diamine (46). ^{1}H NMR (360 MHz, DMSO-d_6) δ 7.35 (d, *J*=2.93 Hz, 1H), 7.20 (d, *J*=7.68 Hz, 1H), 6.87 (t, *J*=5.85 Hz, 1H), 6.54 (d, *J*=8.05 Hz, 1H), 5.99 (d, *J*=2.93 Hz, 1H), 5.86 (s, 1H), 5.39 (s, 2H), 5.35 (s, 2H), 4.61 (d, *J*=5.85 Hz, 2H), 3.71 (d, *J*=2.93 Hz, 6H), 2.31 (s, 3H).^{13}C NMR (91 MHz, DMSO-d_6) δ 167.6, 161.6, 156.7, 151.9, 150.1, 148.5, 143.4, 141.7, 131.6, 117.5, 113.0, 109.0, 100.0, 98.0, 54.2, 51.5, 51.2, 34.0, 10.3. ESI-HRMS (TOF) *m/z*: 396.1787 (Calcd. for $C_{19}H_{21}N_7O_3$ $[M+H]^+$: 396.1784).

5-((6-methoxypyridin-2-yl)methyl)-*N*^{4}-((5-methylisoxazol-3-yl)methyl)-5*H*-pyrrolo[3,2-*d*]pyrimidine-2,4-diamine (47). ^{1}H NMR (400 MHz, DMSO-d_6) δ 7.58-7.65 (m, *J*=8.10 Hz, 1H), 7.36 (d, *J*=2.86 Hz, 1H), 6.90 (t, *J*=5.83 Hz, 1H), 6.69 (d, *J*=8.36 Hz, 1H), 6.50 (d, *J*=7.26 Hz, 1H), 5.99-6.03 (m, 1H), 5.83 (s, 1H), 5.44 (s, 2H), 5.36 (s, 2H), 4.59 (d, *J*=5.72 Hz, 2H), 3.71 (s, 3H), 2.31 (s, 3H).^{13}C NMR (91 MHz, DMSO-d_6) δ 167.7, 162.1, 161.8, 157.0, 154.5, 150.4, 148.8, 139.1, 132.0, 112.8, 109.4, 108.2, 100.2, 98.5, 51.9, 51.9, 34.2, 10.6. ESI-HRMS (TOF) *m/z*: 366.1678 (Calcd. for $C_{18}H_{19}N_7O_2$ $[M+H]^+$: 366.1678).

5-((5-fluoropyridin-2-yl)methyl)-*N*^{4}-((5-methylisoxazol-3-yl)methyl)-5*H*-pyrrolo[3,2-*d*]pyrimidine-2,4-diamine (48). ^{1}H NMR (360 MHz, DMSO-d_6) δ 8.42 (d, *J*=2.93 Hz, 1H), 7.70 (dt, *J*=2.93, 8.78 Hz, 1H), 7.39 (d, *J*=2.93 Hz, 1H), 7.31 (t, *J*=5.67 Hz, 1H), 7.09 (dd, *J*=4.57, 8.60 Hz, 1H), 6.00 (d, *J*=2.93 Hz, 1H), 5.88 (s, 1H), 5.52 (s, 2H), 5.41 (s, 2H), 4.59 (d, *J*=5.85 Hz, 2H), 2.32 (s, 3H).^{13}C NMR (91 MHz, DMSO-d_6) δ 167.6, 161.6, 156.9, 155.7, 152.7, 150.2, 148.6, 135.6, 131.5, 123.3, 121.9, 108.9, 100.1, 98.3, 51.2, 33.8, 10.4. ESI-HRMS (TOF) *m/z*: 354.1480 (Calcd. for $C_{17}H_{16}FN_7O$ $[M+H]^+$: 354.1478).

5-((3-fluoropyridin-2-yl)methyl)-*N*^{4}-((5-methylisoxazol-3-yl)methyl)-5*H*-pyrrolo[3,2-*d*]pyrimidine-2,4-diamine (49). ^{1}H NMR (360 MHz, DMSO-d_6) δ 8.22 (d, *J*=4.76 Hz, 1H), 7.78 (t, *J*=9.25 Hz, 1H), 7.63 (t, *J*=5.58 Hz, 1H), 7.47 (td, *J*=4.35, 8.51 Hz, 1H), 7.26 (d, *J*=3.23 Hz, 1H), 6.06 (s, 1H), 5.97 (d, *J*=2.93 Hz, 1H), 5.58 (d, *J*=1.83 Hz, 2H), 5.39 (s, 2H), 4.63 (d, *J*=5.49 Hz, 2H), 2.34 (s, 3H).^{13}C NMR (91 MHz, DMSO-d_6) δ 167.8, 161.7, 156.9, 150.0, 148.9, 143.8, 143.5, 131.6, 124.5, 123.3, 123.2, 109.6, 100.5, 98.4, 46.7, 34.1, 10.6. ESI-HRMS (TOF) *m/z*: 354.1479 (Calcd. for $C_{17}H_{16}FN_7O$ $[M+H]^+$: 354.1478).

N^4-((5-methylisoxazol-3-yl)methyl)-5-((5-(trifluoromethyl)pyridin-2-yl)methyl)-5*H*-pyrrolo[3,2-*d*]pyrimidine-2,4-diamine (50). ^{1}H NMR (360 MHz, DMSO-d_6) δ 8.85 (s, 1H), 8.17 (dd, *J*=2.20, 8.42 Hz, 1H), 7.41 (d, *J*=2.93 Hz, 1H), 7.10 (t, *J*=5.67 Hz, 1H), 7.02 (d, *J*=8.25 Hz, 1H), 6.05 (d, *J*=2.93 Hz, 1H), 5.74 (s, 1H), 5.69 (s, 2H), 5.43 (s, 2H), 4.56 (d, *J*=5.49 Hz, 2H), 2.28 (s, 3H).^{13}C NMR (91 MHz, DMSO-d_6) δ 167.5, 161.6, 161.2, 157.0, 150.5, 148.6, 144.4, 144.4, 133.8, 133.7, 131.9, 120.0, 109.0, 99.9, 98.7, 51.7, 33.7, 10.3. ESI-HRMS (TOF) *m/z*: 404.1450 (Calcd. for $C_{18}H_{16}F_3N_7O$ $[M+H]^+$: 404.1446).

N^4-((5-methylisoxazol-3-yl)methyl)-5-((4-(trifluoromethyl)pyridin-2-yl)methyl)-5*H*-pyrrolo[3,2-*d*]pyrimidine-2,4-diamine (51). ^{1}H NMR (360 MHz, DMSO-d_6) δ 8.72 (d, *J*=5.12 Hz, 1H), 7.72 (d, *J*=5.12 Hz, 1H), 7.30-7.45 (m, 3H), 6.03 (d, *J*=3.29 Hz, 1H), 5.83 (s, 1H), 5.65 (s, 2H), 5.43 (s, 2H), 4.60 (d, *J*=5.85 Hz, 2H), 2.31 (s, 3H).^{13}C NMR (91 MHz, DMSO-d_6) δ 167.5, 161.6, 158.2, 156.9, 150.3, 149.4, 148.6, 131.7, 117.3, 117.3, 115.9, 115.8, 109.0, 99.9, 98.6, 51.5, 33.8, 10.3. ESI-HRMS (TOF) *m/z*: 404.1451 (Calcd. for $C_{18}H_{16}F_3N_7O$ $[M+H]^+$: 404.1446).

5-((3-chloropyridin-2-yl)methyl)-N^4-((5-methylisoxazol-3-yl)methyl)-5*H*-pyrrolo[3,2-*d*]pyrimidine-2,4-diamine (52). ^{1}H NMR (360 MHz, DMSO-d_6) δ 8.32 (d, *J*=4.76 Hz, 1H), 8.00 (d, *J*=8.05 Hz, 1H), 7.71 (br t, *J*=5.49 Hz, 1H), 7.42 (dd, *J*=4.57, 8.23 Hz, 1H), 7.30 (d, *J*=2.93 Hz, 1H), 6.03 (s, 1H), 5.94-6.00 (m, 1H), 5.62 (s, 2H), 5.44 (s, 2H), 4.62 (d, *J*=5.49 Hz, 2H), 2.34 (s, 3H).^{13}C NMR (91 MHz, DMSO-d_6) δ 167.6, 161.6, 156.7, 152.0, 149.6, 148.7, 146.0, 136.9, 131.7, 128.7, 123.7, 109.7, 100.3, 98.0, 49.4, 33.9, 10.4. ESI-HRMS (TOF) *m/z*: 370.1183 (Calcd. for $C_{17}H_{16}ClN_7O$ $[M+H]^+$: 370.1183).

5-((4-chloropyridin-2-yl)methyl)-*N*^{4}-((5-methylisoxazol-3-yl)methyl)-5*H*-pyrrolo[3,2-*d*]pyrimidine-2,4-diamine (53). ^{1}H NMR (400 MHz, DMSO-d_6) δ 8.41 (d, *J*=5.50 Hz, 1H), 7.48 (dd, *J*=1.87, 5.39 Hz, 1H), 7.36-7.45 (m, 2H), 7.17-7.23 (m, 1H), 6.01 (d, *J*=3.08 Hz, 1H), 5.89 (s, 1H), 5.52 (br s, 2H), 5.38 (br s, 2H), 4.60 (d, *J*=5.72 Hz, 2H), 2.33 (s, 3H).^{13}C NMR (91 MHz, DMSO-d_6) δ 167.7, 161.6, 158.3, 157.0, 150.3, 149.2, 148.7, 142.8, 131.6, 121.9, 120.6, 109.0, 100.1, 98.5, 51.4, 33.9, 10.5. ESI-HRMS (TOF) *m/z*: 370.1183 (Calcd. for $C_{17}H_{16}ClN_7O$ $[M+H]^+$: 370.1183).

4-((5-methylisoxazol-3-yl)methoxy)-5-(pyridin-2-ylmethyl)-5*H*-pyrrolo[3,2-*d*]pyrimidin-2-amine (54). ^{1}H NMR (360 MHz, DMSO-d_6) δ 8.47 (qd, *J*=0.96, 4.80 Hz, 1H), 7.65 (dt, *J*=1.83, 7.68 Hz, 1H), 7.53 (d, *J*=2.93 Hz, 1H), 7.24 (ddd, *J*=1.10, 4.76, 7.68 Hz, 1H), 6.71 (d, *J*=8.05 Hz, 1H), 6.14 (d, *J*=2.93 Hz, 1H), 5.92 (s, 2H), 5.85 (d, *J*=1.10 Hz, 1H), 5.47 (s, 2H), 5.37 (s, 2H), 2.35 (d, *J*=0.73 Hz, 3H).^{13}C NMR (91 MHz, DMSO-d_6) δ 168.4, 158.9, 156.7, 156.7, 153.8, 152.3, 147.8, 135.8, 133.3, 121.1, 119.0, 108.3, 100.0, 98.2, 56.6, 52.2, 10.5. ESI-HRMS (TOF) *m/z*: 337.1416 $[M+H]^+$ (Calcd. for $C_{17}H_{16}N_6O_2$: 337.1413).

4-((5-methyloxazol-2-yl)methoxy)-5-(pyridin-2-ylmethyl)-5*H*-pyrrolo[3,2-*d*]pyrimidin-2-amine (55). ^{1}H NMR (360 MHz, DMSO-d_6) δ 8.43 (br d, *J*=4.39 Hz, 1H), 7.62 (t, *J*=7.83 Hz, 1H), 7.51-7.54 (m, 1H), 7.18-7.25 (m, 1H), 6.82 (s, 1H), 6.74 (d, *J*=7.68 Hz, 1H), 6.13 (d, *J*=2.20 Hz, 1H), 5.89 (s, 2H), 5.43 (s, 2H), 5.39 (s, 2H), 2.24 (s, 3H).^{13}C NMR (91 MHz, DMSO-d_6) δ 156.7, 156.5, 156.5, 156.4, 153.7, 152.4, 148.5, 147.8, 135.6, 133.5, 121.9, 121.2, 119.2, 98.2, 56.8, 52.3, 9.4. ESI-HRMS (TOF) *m/z*: 337.1413 (Calcd. for $C_{17}H_{16}N_6O_2$ $[M+H]^+$: 337.1413).

4-((5-methylthiazol-2-yl)methoxy)-5-(pyridin-2-ylmethyl)-5*H*-pyrrolo[3,2-*d*]pyrimidin-2-amine (56). ^{1}H NMR (360 MHz, DMSO-d_6) δ 8.46 (d, *J*=4.76 Hz, 1H), 7.63 (dt, *J*=1.46, 7.68

Hz, 1H), 7.52 (d, *J*=2.93 Hz, 1H), 7.43 (d, *J*=1.10 Hz, 1H), 7.22 (dd, *J*=4.94, 7.14 Hz, 1H), 6.71 (d, *J*=7.68 Hz, 1H), 6.15 (d, *J*=3.29 Hz, 1H), 5.92 (s, 2H), 5.58 (s, 2H), 5.49 (s, 2H), 2.37 (s, 3H).^{13}C NMR (101 MHz, DMSO-d_6) δ 163.7, 158.3, 158.3, 155.2, 154.2, 149.5, 140.5, 137.4, 135.1, 135.5, 122.8, 120.8, 110.1, 100.0, 63.5, 53.9, 11.8. ESI-HRMS (TOF) *m/z*: 353.1183 $[M+H]^+$ (Calcd. for $C_{17}H_{16}N_6OS$: 353.1184).

4-((5-methyl-1,2,4-oxadiazol-3-yl)methoxy)-5-(pyridin-2-ylmethyl)-5*H*-pyrrolo[3,2-*d*]pyrimidin-2-amine (57). ^{1}H NMR (360 MHz, DMSO-d_6) δ 8.43 (br d, *J*=4.03 Hz, 1H), 7.64 (br t, *J*=7.68 Hz, 1H), 7.53 (d, *J*=2.93 Hz, 1H), 7.16-7.28 (m, 1H), 6.84 (d, *J*=7.68 Hz, 1H), 6.13 (d, *J*=2.93 Hz, 1H), 5.89 (s, 2H), 5.51 (br s, 2H), 5.46 (br s, 2H), 2.54-2.61 (m, 3H).^{13}C NMR (91 MHz, DMSO-d_6) δ 176.0, 165.1, 156.5, 156.3, 153.5, 152.3, 147.6, 135.5, 133.3, 121.0, 119.3, 108.2, 98.1, 55.6, 52.1, 10.6. ESI-HRMS (TOF) *m/z*: 338.1364 (Calcd. for $C_{16}H_{15}N_7O_2$ $[M+H]^+$: 338.1365).

5-((3-methoxypyridin-2-yl)methyl)-4-((5-methyloxazol-2-yl)methoxy)-5*H*-pyrrolo[3,2-*d*]pyrimidin-2-amine (58). ^{1}H NMR (360 MHz, DMSO-d_6) δ 7.87 (dd, *J*=1.10, 4.39 Hz, 1H), 7.37 (d, *J*=2.93 Hz, 1H), 7.33 (dd, *J*=1.10, 8.42 Hz, 1H), 7.21 (dd, *J*=4.76, 8.05 Hz, 1H), 6.80 (d, *J*=1.10 Hz, 1H), 6.07 (d, *J*=2.93 Hz, 1H), 5.80 (s, 2H), 5.45 (s, 2H), 5.32 (s, 2H), 3.77 (s, 3H), 2.22 (d, *J*=1.10 Hz, 3H).^{13}C NMR (91 MHz, DMSO-d_6) δ 156.4, 156.3, 153.7, 152.0, 150.9, 148.4, 144.7, 138.8, 133.6, 122.0, 121.8, 116.2, 108.9, 97.5, 56.6, 54.2, 47.2, 9.3. ESI-HRMS (TOF) *m/z*: 367.1520 (Calcd. for $C_{18}H_{18}N_6O_3$ $[M+H]^+$: 367.1518).

5-((3-methoxypyridin-2-yl)methyl)-4-((5-methylisoxazol-3-yl)methoxy)-5*H*-pyrrolo[3,2-*d*]pyrimidin-2-amine (59). ^{1}H NMR (360 MHz, DMSO-d_6) δ 7.89 (d, *J*=4.39 Hz, 1H), 7.32-7.43 (m, 2H), 7.24 (dd, *J*=4.76, 8.05 Hz, 1H), 6.06 (d, *J*=2.56 Hz, 1H), 5.82 (br s, 2H), 5.77 (br s,

1H), 5.47 (s, 2H), 5.30 (s, 2H), 3.79 (s, 3H), 2.35 (s, 3H).^{13}C NMR (91 MHz, DMSO-d_6) δ 168.4, 159.0, 156.4, 153.8, 152.0, 151.0, 144.8, 138.9, 133.5, 122.1, 116.3, 109.0, 99.9, 97.6, 56.5, 54.2, 47.3, 10.6. ESI-HRMS (TOF) *m/z*: 367.1519 (Calcd. for $C_{18}H_{18}N_6O_3$ $[M+H]^+$: 367.1518).

ASSOCIATED CONTENT

Supporting Information. Experimental details, docking methods, biological assay details, and molecular formula strings can be found in the supporting information. This material is available free of charge via the Internet at http://pubs.acs.org

AUTHOR INFORMATION

Corresponding Authors

*D. McGowan. +32 6414 1019, dmcgowan@its.jnj.com

*F. Herschke. +32 6414 1644, fherschk@its.jnj.com

ACKNOWLEDGMENT

With thanks to Eddy De Wilde, Kristien Raeymaekers, Michel Carpentier, Alex De Groot, Hilde Verheyen, and Alberto Fontana for analysis and purification, and Monicah Otieno for bioanalysis.

ABBREVIATIONS

HBV, Hepatitis B Virus; TLR, Toll-like Receptor; IFN, interferon; TNF, tumor necrosis factor; NF-κB, Nuclear factor-κB; pDC, plasmacytoid dentritic cells; ISG, Interferon stimulated genes; PBMC, peripheral blood mononuclear cells.

Authors will release the atomic coordinates and experimental data upon article publication.

REFERENCES

(1) Dienstag, J. L. Hepatitis B virus infection. *New Engl. J. Med.* **2008,** *359*, 1486-1500.

(2) World Health Organization. *Guidelines for the prevention, care, and treatment of persons with chronic hepatitis B infection*; Geneva, Switzerland, 2015. ISBN 978 92 4 154905 9

(3) Chang, T.-T.; Gish, R. G.; de Man, R.; Gadano, A.; Sollano, J.; Chao, Y.-C.; Lok, A.; Han, K.-H.; Goodman, Z.; Zhu, J.; Cross, A.; DeHertogh, D.; Wilber, R.; Colonno, R.; Apelian, D. A Comparison of entecavir and lamivudine for HBeAg-positive chronic hepatitis B. *New Engl. J. Med.* **2006**, *354*, 1001-1010.

(4) Perrillo, R. Benefits and risks of interferon therapy for hepatitis B. *Hepatol.* **2009**, *45*, S103-S111.

(5) Terrault, N.A.; N.H.; Bzowej, N.H.; Chang, K.-M.; Hwang, J.P.; Jonas, M.M.; Murad, M.H. AASLD guidelines for treatment of chronic hepatitis B. *Hepatology*, **2016**, *63*, 261-283.

(6) Protzer, U.; Maini, M. K.; Knolle, P. A. Living in the liver: hepatic infections. *Nat. Rev. Immunol.* **2012**, *12*, 201-213.

(7) Chan, H. L.; Thompson, A.; M.-Peignoux, M.; Piratvisuth, T.; Cornberg, M.; Brunetto M. R.; Tillmann, H.L.; Kao, J.H.; Jia, J.D.; Wedemeyer, H.; Locarnini, S.; Janssen, H.L.; Marcellin, P. Hepatitis B surface antigen quantification: why and how to use it in 2011 - A core group report. *J. Hepatol.* **2011**, *55*, 1121-1131.

(8) Schoggins, J. W. Interferon-stimulated genes: roles in viral pathogenesis. *Curr Opin Virol.* **2014**, *6*, 40-46.

(9) Yokosuka, O.; Omata, M.; Imazeki, F.; Okuda, K.; Summers, J. Changes of hepatitis B virus DNA in liver and serum caused by recombinant leukocyte interferon treatment: analysis of intrahepatic replicative hepatitis B virus DNA. *Hepatology* **1985**, *5*, 728-734.

(10) Santini, S. M.; Lapenta, C.; Logozzi, M.; Parlato, S.; Spada, M.; Di Pucchio, T.; Belardelli, F. Type I interferon as a powerful adjuvant for monocyte-derived dendritic cell development and activity in vitro and in Hu-PBL-SCID mice. *J. Exp. Med*. **2000**, *191*, 1777-1788.

(11) Roethle, P. A.; McFadden, R. M.; Yang, H.; Hrvatin, P.; Hui, H.; Graupe, M.; Gallagher, B.; Chao, J.; Hesselgesser, J.; Duatschek, P.; Zheng, J.; Lu, B.; Tumas, D. B.; Perry, J.; Halcomb, R. L. Identification and optimization of pteridinone toll-like receptor 7 (TLR7) agonists for the oral treatment of viral hepatitis. *J. Med. Chem.* **2013**, *56*, 7324-7333.

(12) Akira, S.; Hemmi, H. Recognition of pathogen-associated molecular patterns by TLR family *Immunol. Lett.* **2003**, *85*, 85-95.

(13) Pasare, C.; Medzhitov, R. Toll-like receptors: linking innate and adaptive immunity. *Microbes and Infection* **2004**, *6*, 1382–1387.

(14) Akira, S.; Takeda, K.; Kaisho, T. Toll-like receptors: Critical proteins linking innate and acquired immunity. *Nat. Imm. Rev.* **2001**, *2*, 675-680.

(15) Jurk, M.; Heil, F.; Vollmer, J.; Schetter, C.; Krieg, A.; Wagner, H.; Lipford, G.; Bauer, S. Human TLR7 or TLR8 independently confer responsiveness to the antiviral compound R-848. *Nat. Immunol.* **2002**, *3*, 499.

(16) Hemmi, H.; Kaisho, T.; Takeuchi, O.; Sato, S.; Sanjo, H.; Hoshino, K.; Horiuchi, T.; Tomizawa, H.; Takeda, K.; Akira, S. Small anti-viral compounds activate immune cells via the TLR7 MyD88-dependent signaling pathway *Nat. Immunol.* **2002**, *3*, 196-200

(17) Hanten, J. A.; Vasilaskos, J. P.; Riter, C.L.; Neys, L.; Lipson, K.E.; Alkan, S.S., Birmachu, W. Comparison of human B cell activation by TLR7 and TLR9 agonists. *BMC Immunology* **2008**, *9*, 39. doi:10.1186/1471-2172-9-39

(18) Vanwolleghem, T.; Hou, J.; van Oord, G.; Andeweg, A.C.; Osterhaus, A.D.; Pas, S.D.; Janssen, H.L.; Boonstra, A. Re-evaluation of hepatitis B virus clinical phases by systems biology identifies unappreciated roles for the innate immune response and B cells. *Hepatology* **2015**, *62*, 87-100.

(19) Bekeredjian-Ding I.; Roth, S.I.; Gilles, S.; Giese, T.; Ablasser, A.; Hornung, V.; Endres, S.; Hartmann, G. T Cell-Independent, TLR-induced IL-12p70 production in primary human monocytes. *J. Immunol.* **2006**, *176*, 7438-7446.

(20) Gorden, K. B.; Gorski, K. S.; Gibson, S. J.; Kedl, R. M.; Kieper, W. C.; Qiu, X.; Tomai, M. A.; Alkan, S.S.; Vasilakos, J. P. Synthetic TLR agonists reveal functional differences between human TLR7 and TLR8. *J. Immunol.* **2005**, *174*, 1259-1268.

(21) (a) Isobe, Y.; Kurimoto, A.; Tobe, M.; Hashimoto, K.; Nakamura, T.; Norimura, K.; Ogita, H.; Takaku, H. Synthesis and biological evaluation of novel 9-substituted-8-

hydroxyadenine derivatives as potent interferon inducers *J. Med. Chem.* **2006**, *49*, 2088-2095. (b) Koga-Yamakawa, E.; Dovedi, S. J.; Murata, M.; Matsui, H.; Leishman, A. J.; Bell, J.; Ferguson, D.; Heaton, S. P.; Oki, T.; Tomizawa, H.; Bahl, A.; Takaku, H.; Wilkinson, R. W.; Harada, H. Intratracheal and Oral Administration of SM-276001: A selective TLR7 agonist, leads to antitumor efficacy in primary and metastatic models of cancer. *Int. J. Cancer* **2013**, *132*, 580-590.

(22) (a) Miller, R. L.; Gerster, J. F.; Owens, M. L.; Slade, H. B.; Tomai, M. A.; Imiquimod applied topically: a novel immune response modifier and a new class of drug. *Intl. J. Immunopharmacol.* **1999**, *21*, 1-14. (b) Gerster, J. F.; Lindstrom, K. J.; Miller, R. L.; Tomai, M. A.; Birmachu, W.; Bomersine, S. N.; Gibson, S. J.; Imbertson, L. M.; Jacobson, J. R.; Knafla, R. T.; Maye, P. V.; Nikolaides, N.; Oneyemi, F.Y.; Parkhurst, G. J.; Pecore, S. E.; Reiter, M. J.; Scribner, L. S.; Testerman, T. L.; Thompson, N. J.; Wagner, T. L.; Weeks, C. E.; Andre, J. D.; Lagain, D.; Bastard, Y.; Lupu, M. Synthesis and structure-activity relationships of 1*H*-imidazo[4, 5-*c*]quinolines that induce interferon production. *J. Med. Chem.* **2005**, *48*, 3481−3491.

(23) Fosdick, A.; Zheng, J.; Pflanz, S.; Frey, C. R.; Hesselgesser, J.; Halcomb, R. L.; Wolfgang, G.; Tumas, D. B. Pharmacokinetic and pharmacodynamic properties of GS-9620, a novel toll-like receptor 7 agonist, demonstrate interferon-stimulated gene induction without detectable serum interferon at low oral doses. *J. Pharmacol. Exp. Ther.* **2014**, *348*, 96-105.

(24) Tumas, D.; Zheng, X.; Rhodes, G.; Duatschek, P.; Hesselgesser, J.; Frey, C.; Henne, I.; Fosdick, A.; Halcomb, R.; Wofgang, G. Preclinical characterization of GS-9620, a potent and selective oral TLR7 agonist. *J. Hepatol.* **2011**, *54*, S446-S447.

(25) McGowan, D. C.; Herschke, F.; Pauwels, F.; Stoops, B.; Last, S.; Pieters, S.; Scholliers, A.; Thoné, T.; Van Schoubroeck, B.; De Pooter, D.; Mostmans, W.; Khamlichi, M., D.; Embrechts, W.; Dhuyvetter, D.; Smyej, I.; Arnoult, E.; Demin, S.; Borghys, H.; Fanning, F.; Vlach, J.; Raboisson P. Novel pyrimidine toll-like receptor 7 and 8 dual agonists to treat hepatitis B virus, *J. Med. Chem.* **2016**, *59*, 7936–7949.

(26) (a) Bennett, N. J.; McInally, T.; Mochel, T.; Thom, S.; Tidén, A.-K. Pyrimidine derivatives for the treatment of asthma, COPD, allergic rhinitis, allergic conjunctivitis, atopic dermatitis, cancer, hepatitis B, hepatitis C, HIV, HPV, bacterial infections and dermatosis. WO2009067081, **2009**. (b) Tosaki, S.; Hori, S. Cyclic amide compounds and their use in the treatment of disease. WO2012067268, **2012**.

(27) Lanford, R. E.; Guerra, B.; Chavez, D.; Giavedoni, L.; Hodara, V. L.; Brasky, K. M.; Fosdick, A.; Frey, C. R.; Zheng, J.; Wolfgang, G.; Halcomb, R. L.; Tumas, D. B. GS-9620, an oral agonist of toll-like receptor-7, induces prolonged suppression of hepatitis B virus in chronically infected chimpanzees. *Gastroenterology* **2013**, *144*, 1508−1517.

(28) Borovik, V. P.; Shkurko, O. P. Synthesis of functional 2-substituted 4-phenyl-9*H*-pyrimido[4,5-*b*]indoles. *Russ. Chem. Bull., Intl. Ed.* **2002**, *51*, 2129-2133.

(29) (a) Bräse, S.; Gil, C.; Knepper, K.; Zimmermann, V. Organic Azides: An exploding diversity of a unique class of compounds. *Angew. Chem. Int. Ed*. **2005**, *44*, 5188-5240. (b)

Kolb, H. C.; Finn, M. G.; Sharpless, K. B. Click chemistry: Diverse chemical function from a few good reactions. *Angew. Chem. Int. Ed.* **2001**, *40*, 2004-2021.

(30) (a) Elliott, A. J.; Montgomery, J. A.; Walsh, D. A. A short, facile synthesis of 2-amino-1,5-dihydro-4*H*-pyrrolo[3,2-*d*]-pyrimidin-4-one (9-deazaguanine) *Tet. Lett.* **1996**, *37*, 4339-4340. (b) Elliott, A. J.; Morris, P. E.; Petty, S. L.; Williams, C. H. An improved synthesis of 7-substituted pyrrolo[3,2-*d*]pyrimidines. *J. Org. Chem.* **1997**, *62*, 8071-8075. (c) Theoclitou, M.; Aquila, B.; Block, M. H.; Brassil, P. J.; Castriotta, L.; Code, E.; Collins, M. P.; Davies, A. M.; Deegan, T.; Ezhuthachan, J.; Filla, S.; Freed, E.; Hu, H.; Huszar, D.; Jayaraman, M.; Lawson, D.; Lewis, P. M.; Nadella, M. V. P.; Oza, V.; Padmanilayam, M.; Pontz, T.; Ronco, L.; Russell, D.; Whitston, D.; Zheng, X. J. Discovery of (+)-*N*-(3-aminopropyl)-*N*-[1-(5-benzyl-3-methyl-4-oxo-[1,2]thiazolo[5,4-*d*]-pyrimidin-6-yl)-2-methylpropyl]-4-methylbenzamide (AZD4877), a kinesin spindle protein inhibitor and potential anticancer agent. *J. Med. Chem.* **2011**, *54*, 6734−6750.

(31) Brown, D. G.; Maier, D. L.; Sylvester, M. A.; Hoerter, T. N.; Menhaji-Klotz, E.; Lasota, C. C.; Hirata, L. T.; Wilkins, D.E.; Scott, C. W.; Trivedi, S.; Chen, T.; McCarthy, D. J.; Maciag, C. M.; Sutton, E. J.; Cumberledge, J.; Mathisen, D.; Roberts, J.; Gupta, A.; Liu, F.; Elmore, C. S.; Alhambra, C.; Krumrine, J. R.; Wang, X.; Ciaccio, P. J.; Wood, M. W.; Campbell, J. B.; Johansson, M. J.; Xia, J.; Wen, X.; Jiang, J.; Wang, X.; Peng, Z.; Hu, T.; Wang, J. 2,6-Disubstituted pyrazines and related analogs as NR2B site antagonists of the NMDA receptor with anti-depressant activity. *Bioorg. Med. Chem. Lett.* **2011**, *21*, 3399-3403.

(32) Carvalho, J. F.; Louvel, J.; Doornbos, M. L.; Klaasse, E.; Yu, Z.; Brussee, J.; Ijzerman, A. Strategies to reduce hERG K+ channel blockade. Exploring heteroaromaticity and rigidity in novel analogues of Dofetilide. *J. Med. Chem.* **2013**, *56*, 2828-2840.

(33) Jamieson, C.; Moir, E. M.; Rankovic, Z.; Wishart, G. Medicinal chemistry of hERG optimizations: Highlights and hang-ups. *J. Med. Chem.* **2006**, *49*, 5029-4046.

(34) Zhang, Z.; Ohto, U.; Shibata, T.; Krayukhina, E.; Taoka, M.; Yamauchi, Y.; Tanji, H.; Isobe, T.; Uchiyama, S.; Miyake, K.; Shimizu1, T. *Immunity* **2016**, *45*, 737–748.

(35) Mathes, C. QPatch: the past, present and future of automated patch clamp. *Exp. Op. Ther. Targets* **2006**, *10*, 319-327. doi:10.1517/14728222.10.2.319

(36) Huang, L.-R.; Wu, H.-L.; Chen, P.-J.; Chen, D.-S. An immunocompetent mouse model for the tolerance of human chronic hepatitis B virus infection. *Proc. Natl. Acad. Sci.* **2006**, *103*, 17862–17867.

(37) Ketloy, C.; Engering, A.; Srichairatanakul, U.; Limsalakpetch, A.; Yongvanitchit, K.; Pichyangkul, S.; Ruxrungtham, K. Expression and function of toll-like receptors on dendritic cells and other antigen presenting cells from non-human primates. *Vet. Immunol. Immunopathol.* **2008**, *125*, 18-30.

(38) Starkhammar, M.; Larsson, O.; Georén, S. K.; Leino, M.; Dahlén, S.-E., Adner, M.; Cardell, L.-O. Toll-like receptor ligands LPS and Poly (I:C) exacerbate airway hyperresponsiveness in a model of airway allergy in mice, independently of inflammation. PLoS ONE **2014**, *9*, e104114. doi:10.1371/journal.pone.0104114.

(39) Ronit, A; Plovsing, R.R.; Gaardbo, J.C.; Berg, R.M.; Hartling, H.J.; Ullum, H.; Andersen, Å.B.; Madsen, H.O.; Møller, K.; Nielsen, S.D. Inflammation-induced changes in circulating T-cell subsets and cytokine production during human endotoxemia. *J Intensive Care Med.* **2015**, doi: 10.1177/0885066615606673

(40) Baenziger, S.; Heikenwalder, M.; Johansen, P.; Schlaepfer, E.; Hofer, U.; Miller, R. C.; Diemand, S.; Honda, K.; Kundig, T. M.; Aguzzi, A.; Speck, R. F. Triggering TLR7 in mice induces immune activation and lymphoid system disruption, resembling HIV-mediated pathology. *Blood* **2009**, *8*, 377-388. doi: 10.1182/blood-2008-04-151712.

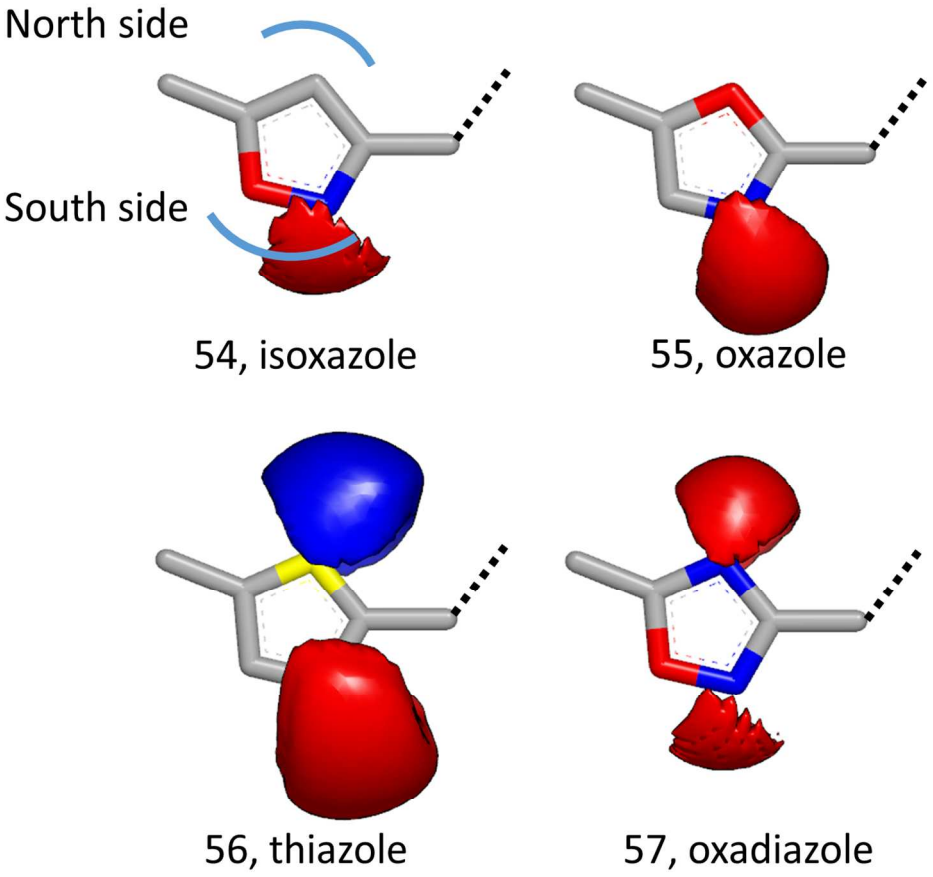

Figure 2 Calculation

129x121mm (300 x 300 DPI)

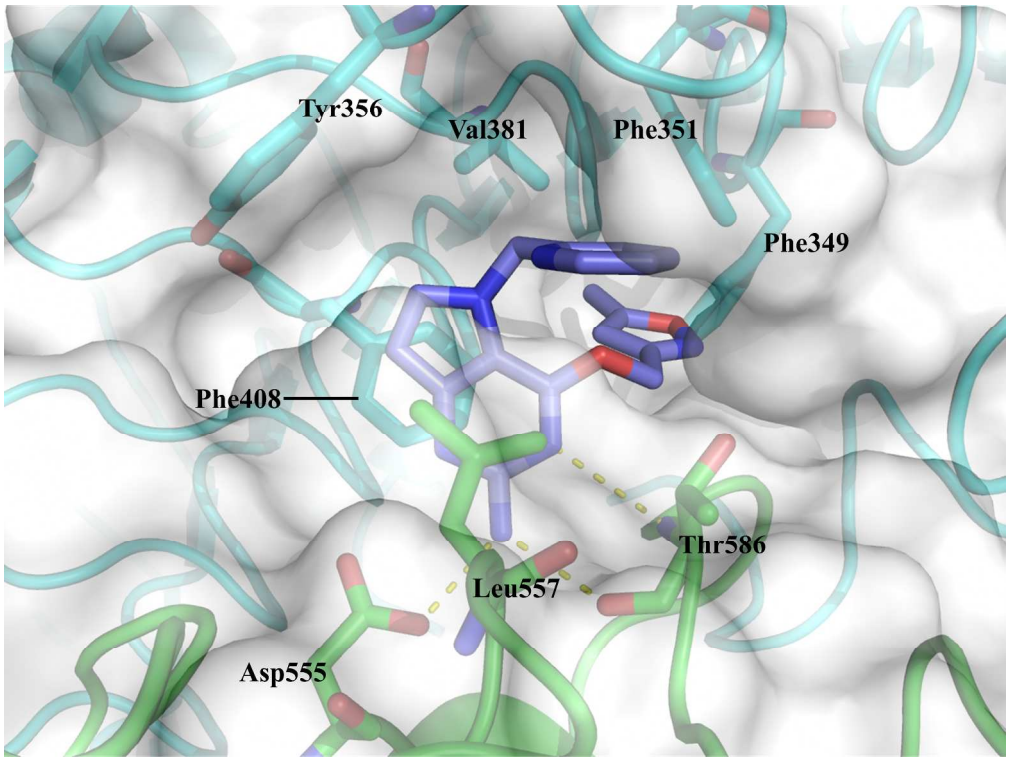

Figure 2. Compound 54 - monkey-TLR7

254x190mm (300 x 300 DPI)

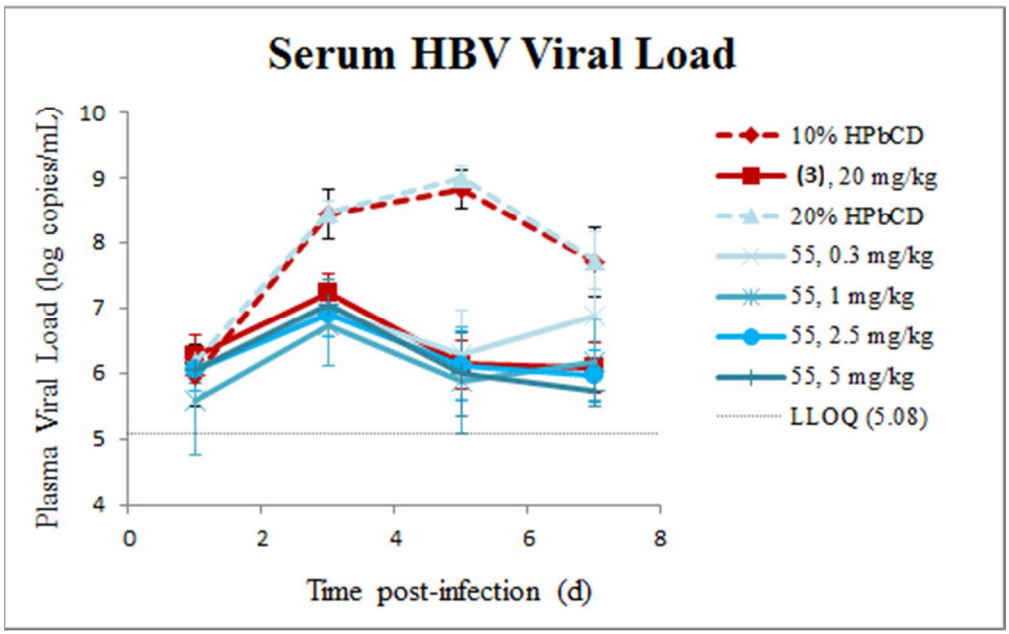

Fig 3a Serum HBV

137x85mm (96 x 96 DPI)

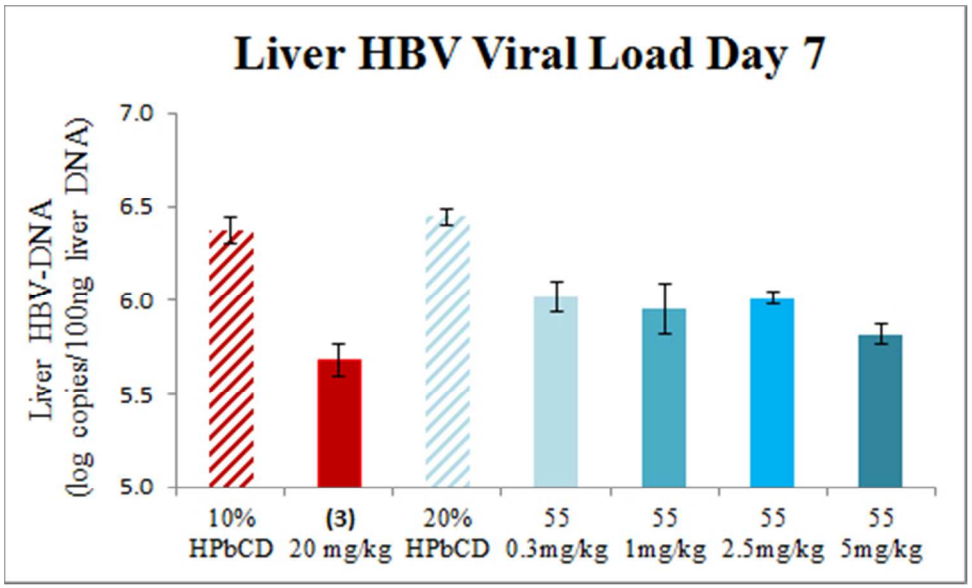

Fig 3b Liver Viral Load

127x76mm (96 x 96 DPI)

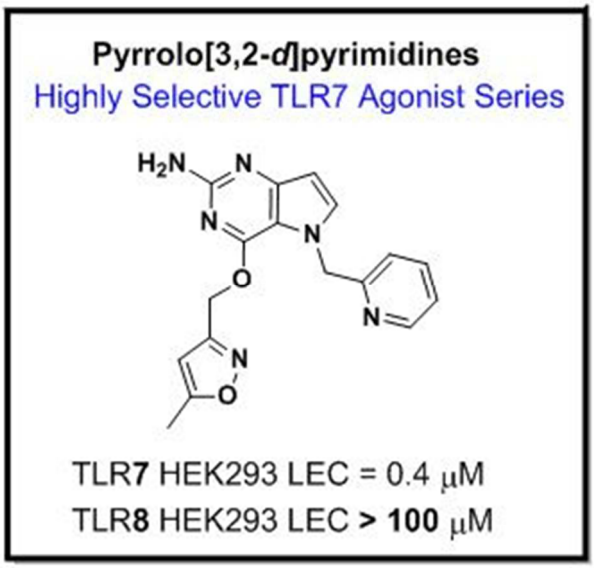

Table of Contents graphic

80x76mm (96 x 96 DPI)